**Addis Ababa University**

**School of Graduate Studies**

**Faculty of Science**

# GIS-Based Conservation Priority Area Identification in Mojo River Watershed On the Basis of Erosion Risk

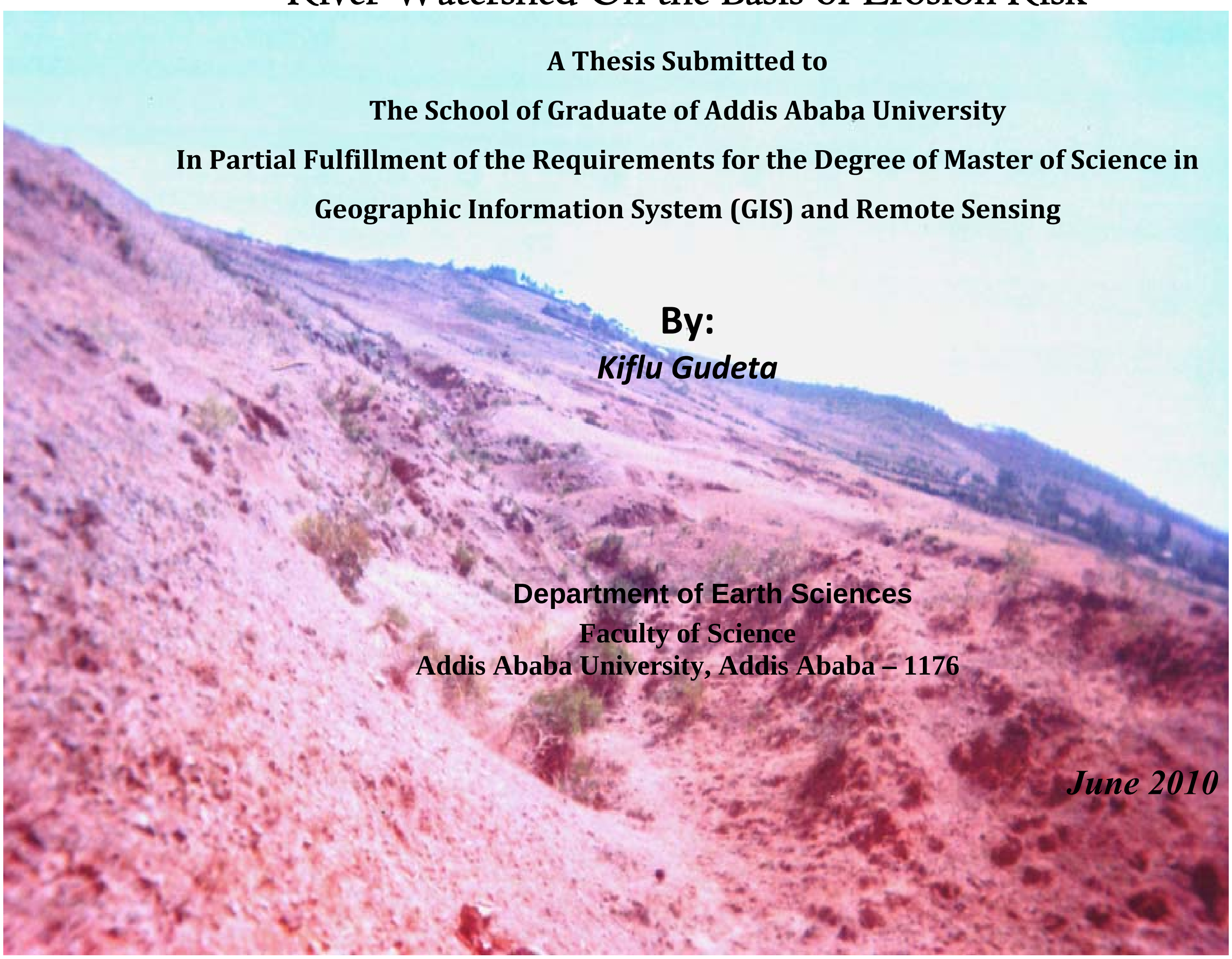

**A Thesis Submitted to**

**The School of Graduate of Addis Ababa University**

**In Partial Fulfillment of the Requirements for the Degree of Master of Science in Geographic Information System (GIS) and Remote Sensing**


**By:**

***Kiflu Gudeta***

**Department of Earth Sciences**
**Faculty of Science**
**Addis Ababa University, Addis Ababa – 1176**


***June 2010***

# Addis Ababa University
# School of Graduate Studies
# Faculty of Science

# GIS-Based Conservation Priority Area Identification in Mojo River Watershed On the Basis of Erosion Risk

**A Thesis Submitted to**

**The School of Graduate of Addis Ababa University**

**In Partial Fulfillment of the Requirements for the Degree of Master of Science in GIS and Remote Sensing**

Under the guidance of

**Dr. Mekuria Argaw (PhD)**

Department of Environmental Science

Addis Ababa University, Addis Ababa

**By:**

***Kiflu Gudeta***

***June 2010***

ADDIS ABABA UNIVERSITY

**SCHOOL OF GRADUATE STUDIES**

# GIS-Based Conservation Priority Area Identification in Mojo River Watershed On the Basis of Erosion Risk

By

Kiflu Gudeta

Faculty of Natural Science

Department of Earth Sciences

Remote Sensing and GIS

## Approval by Board of Examiners

**Dr. Balemual Atnafu** ____________________________

Chairman, Department

Graduate Committee

**Dr. Mekuria Argaw** ____________________________

Advisor

**Prof.Tenalem Ayenew** ____________________________

Examiner

**Dr. K.V. Suryabhagavan** ____________________________

Examiner

## Acknowledgments

First and foremost, Glory be to the Merciful and Almighty God and His Mother, Saint Virgin Mary, for all things done for me in my entire life.

I am greatly indebted to my advisor Dr. Mekuria Argaw whose compassionate guidance and constant encouragement helped me to complete the present research work. He is the person who has always helped me. His constant encouragement made me strong enough to face ups and downs with confidence during the present research study.

I would like to extend my deepest gratitude to Dr. Lulseged Tamene for his constructive advice and guidance. He is also a person who benevolently provided me with invaluable information and relevant literatures for the research work. I am also grateful to Dr. K.V. Suryabhagavan and Dr. Dagnachew Legesse for their guidance, advice, encouragement and support throughout my academic career.

I wish to express my genuine thanks to Horn of Africa regional environment program for granted me financial support for the research work. I am also thankful to AAU Earth Science department, Ministry of Water Resources, National Meteorological Service Agency (NMSA), Central Statistics Agency (CSA), GeoMark systems plc, Lome and Ada'a wereda agricultural offices from where I received all kinds of resource support.

Words cannot express my feelings which I have for my family: Etenesh Tesfaye (Mom), Tesfaye Ali and Ali Shibeshi. I am highly indebted to them for their blessing, guidance, advice, encouragement and support.

Finally, I would like to convey my special thanks to my friends: Senait Dereje (Sunny), Ephrem Haile, Habtamu Mohammed, Yosef Alemayehu, Afework Mekeberia, Ashenafi Burka, Ermias Teferi, Zemenu Mintesinot, and many others for their unforgettable encouragement and help.

# Table of Contents

## List of Figures

## List of Tables

## List of Abbreviations

| | |
|---|---|
| **AAU** | Addis Ababa University |
| **AHP** | Analytical Hierarchy Process |
| **CEI** | Composite Erosion Index |
| **CSA** | Central Statistics Agency |
| **DEM** | Digital Elevation Model |
| **ENVI** | Environment for Visualizing Image |
| **ERDAS** | Earth Resources Data Analysis System |
| **ETM+** | Enhanced Thematic Mapper Plus |
| **FAO** | Food and Agricultural Organization |
| **GIS** | Geographic Information System |
| **GPS** | Global Positioning System |
| **LULC** | Land Use Land Cover |
| **LSMA** | Linear Spectral Mixture Analysis |
| **MCA** | Multi Criteria Analysis |
| **MCDA** | Multi-criteria Decision Analysis |
| **MCE** | Multi Criteria Evaluation |
| **MLC** | Maximum Likelihood Classifier |
| **MoWR** | Ministry Of Water Resources |
| **NDVI** | Normalized Difference Vegetation Index |
| **NMA** | National Meteorological Agency |
| **RS** | Remote Sensing |
| **RUSLE** | Revised Universal Soil Loss Equation |
| **SCRP** | Soil Conservation Research Project |
| **SRTM** | Shuttle Radar Topographic Mission |
| **SPI** | Stream Power Index |
| **WI** | Wetness Index |

## Abstract

*The identification of priority areas for the establishment of control measures is one of the first objectives of conservation plans. Since it is not possible to launch watershed management projects all over the watershed at the same time, it is very important to use some method to prioritize micro-watersheds. A particular sub-watershed may get top priority due to various reasons but often, the intensity of land degradation is taken as the basis. In this study, prioritization of micro-watersheds has been done on the basis of soil erosion risk. A methodology, based on Revised Universal Soil Loss Equation (RUSLE) and Multi-criteria Analysis (MCA), has been applied using remotely sensed data, together with other ancillary data in a GIS environment. The analysis shows that RUSLE and MCA help to categorize landscape units into different levels of erosion risk and identify areas that require priority in conservation measures in relative to others. Based on the RUSLE model, the potential average annual soil loss of each parcel of land in the watersheds ranges from 8.57 to 134.46t/ha/year with a mean annual soil loss of 21.2t/ha/year. The result showed that very high soil loss (82.6- 134.5/ha/yr) is observed in MW6 and Six MWs (7, 9, 12, 14, 20, and 25) fell under high soil erosion classes (59.9 - 82.6t/ha/yr). About 40% of the micro-watersheds fall in below the annual average soil loss of the entire watershed. Based on the MCA approach, micro-watershedwise Composite Erosion Index (CEI) indicates that only MW 6 is under 'Very high' category with mean CEI above 2.11. The area covered under this category is 60.75 Km$^2$ (3.69%). 'High' category is represented by 9 MWs (29.09%) covering 478.77 Km$^2$ area. The landscape positions where steep slope, poor surface cover, erodible soil and gully erosion coincided show high erosion risk compared to others. As a result the critical micro-watersheds which are under very high and high category were selected and recommended to be intervened for conservation measures to reduce on-site soil loss and their off-site effects.*


***Keywords**: GIS, Remote Sensing, Priority area, RUSLE, MCA, Mojo River watershed.*

# 1 INTRODUCTION

## *1.1 General Background*

Land degradation, a decline in land quality, is a serious threat to the prosperity of rural population in the world (Eswaran, *et al.,* 2001). It has negative effects on the standard of living of the inhabitants, especially in developing countries like Ethiopia, where agriculture is considered as the main source of peoples' income and food (Hurni, 1993).

Soil erosion is the most serious form of land degradation, in which its on-site and off-site effects threaten the food security and the national economy of the country (Hurni, 1993; Sutcliff, 1993; Lulseged and Vlek, 2005). According to the Ethiopian highland reclamation study (FAO 1984), in mid 1980's 27 million hectare or almost 50% of the highland area was significantly eroded, 14 million hectare seriously eroded and over 2 million hectare beyond reclamation. In areas such as Wolo, Tigray and Harerge, 50% of the agricultural lands have soils with depth less than 10 cm, which make them unsuitable for farming. As a consequence of soil degradation, the production capacity of soils in the Ethiopian highlands is believed to be undermined at a rate of 2-3% annually (Hurni, 1993). Apart from the adverse effects on the productivity of the land, soil erosion also inflicts offsite costs through the process of sedimentation thereby adversely affecting irrigation and power potential. Sedimentation in Koka hydropower dam, for instance, is causing potential storage capacity loss and thereby an energy loss of 128 M KWh with economic loss over 60 million Birr/year (EEPC, 2002).

To undertake corrective measures and prevent further degradation of many watersheds, timely information on the extent and spatial distribution of erosion areas is of paramount importance. This information is necessary for cost effective soil conservation planning. In a watershed management programme, however, it may not be possible to restore all degraded areas at once due to spatial variability in erosion severity and financial constraints. Therefore, it is necessary to focus watershed restoration efforts on selected watershed priority areas which need immediate attention and where there is hope of making a meaningful difference (Tripathi *et al.,* 2003). This can be a major step in enabling the community to minimize both on-site and off-site effects of land degradation in the long run. To achieve this, various erosion models and/or multi-criteria evaluation approach have been successfully used in various studies (Deore, 2005; Li *et al.,* 1996).

Under these circumstances, Remote Sensing (RS) and Geographical Information System (GIS) become valuable tools to achieve more satisfactory results in the assessment of the soil erosion. RS has been used to identify and map erosion areas (De Asis *et al*., 2008). GIS has made a tremendous impact in many fields of application, because it allows ease of data update, data management and data presentation in forms most suited to user requirements. At the same time, GIS allows for vast amounts of information on different themes and from different sources to be integrated (Shi *et al.*, 2004).

## *1.2 Problem Statement and Justification of the Study*

Ethiopia is currently faced with a number of environmental concerns resulting directly or indirectly from agriculture and exploitation of natural resource base. Mojo River Watershed, the study area, is characterized by a serious soil erosion problem inducing heavy silt loads in rivers (Eyasu, 2003). Lack of vegetation cover associated with other erosion induced factors is exposing the area to high rates of soil erosion and loss of soil fertility. From previous studies the average annual soil loss in the area is 200-300 t/ha (PDRE, 1989). Off-site effects of soil erosion are also the major negative environmental externality affecting the welfare of the rest of the society in the area. This is manifested in the form of sedimentation of hydroelectric dams, pollution of municipal water reservoirs and flooding hazards.

Problems associated with sediment accumulation in the low lying areas are recognized in the study area. For instance, siltation in the Koka reservoir has been an on-going problem since its first impoundment and is posing a major threat to the nation's hydropower generation capacity. According to Eyasu (2003), the rate of siltation in the reservoir has grown from 857t/km$^2$ in 1970 to 2115t/km$^2$/yr. This situation has lowered water volume from the designed live storage capacity of 1,667 Mm$^3$ in 1959 to 1,186 Mm$^3$ in 1998, which is a loss of 30% of the total storage volume of the reservoir (EEPC, 2002). The source of the sediments is believed to be from poorly managed agricultural lands in the headwater watersheds.

As the problems are therefore multi-dimensional and complex, they deserve carefully designed approaches to combat the situation effectively. Previous studies conducted in the area recommended watersheds protection and conservation-based farming to address those on-site and off-site effects of soil erosion (Eyasu, 2003). Because of differences in environmental attributes across landscapes, however, a few areas of the watershed are critical and responsible for high amount of soil losses and sediment delivery. In addition, limited financial resources as well as restrictions on land often exclude the application of conservation measures to all areas experiencing erosion (Tamene and Vlek, 2007). Consequently, identification of hot-spot areas of erosion and prioritizing areas of intervention is extremely important for reducing further degradation, reclaiming the degraded areas and improving the land productivity of the watershed (Lulseged and Vlek, 2005).

Thus, the present study will attempt to identify conservation priority areas in Mojo River Watershed on the basis of erosion risk using Revised Universal Soil loss Equation (RUSLE) model and multi-criteria evaluation (MCE) approach. To achieve this, the analysis used the climatological (rainfall erosivity), pedological (soil erodibility), topographic (slope length and steepness), anthropogenic (ground cover) parameters which are further supported by potential location for gully formation.

## *1.3 Objectives*

### 1.3.1 General Objective

The main objective of this study is to identify priority areas for conservation intervention and restoration measures in Mojo River Watershed using Revised Universal Soil Loss Equation (RUSLE) and multi-criteria evaluation (MCE).

### 1.3.2 Specific Objectives

This study is designed to realize the following specific objectives

- To estimate potential soil loss in the study area using RUSLE model
- To identify potential locations for ephemeral gully formation
- To identify high erosion risk areas (erosion hotspots) in the watershed
- To prioritize micro-watersheds on the basis of erosion risk

## *1.4 Research Questions*

- What is the mean annual rate of soil loss in Mojo River Watershed?
- Where does most severe accelerated soil erosion occur?
- At what locations of the watershed can ephemeral gullies potentially be formed?
- Based on multi-criteria analysis, which micro-watersheds are more prone to soil erosion?
- Which areas of the watersheds need to be given highest priority for conservation measures?

# 2 LITERATURE REVIEW

## *2.1 Watershed Based Management*

Land resource development programmes are applied generally on a watershed basis (Khan *et al*., 2001). Watersheds have been identified as fundamental planning units for the management of land and water resources, particularly in the fragile and heterogeneous erosion-susceptible hilly ecosystems (Doere, 2005). The concept of watershed management recognizes the inter-relationships between landuse, soil and water and the linkage between uplands and downstream areas (Khan *et al*., 2001). Soil and water conservation are key issues in watershed management while demarcating watershed.

While considering watershed conservation work, it is not feasible to take the whole area at once. Thus the whole basin is divided into several smaller management units, as watersheds or sub-watersheds. These management units vary in size, and often require different levels of assessment and planning activities. Watershed delineation is the hydrologic division of a watershed into sub-watersheds that are relatively homogeneous (Alarcon *et al.,* 2006). Although land use and other factors play an important role within the process of delineating a watershed, topography is used as the primary reference. Until recently, watersheds were delineated from relief information (contour lines) on topographic maps or from aerial photo interpretation (Marti'nez-Casasnovas and Stuiver, 1998). Since the advent of GIS, this conventional cartographic representation of topography has been gradually replaced by digital elevation models (DEMs). With the widespread availability of digital elevation databases, watershed delineation has been automated in many GIS/hydrologic software (Alarcon *et al.,* 2006).

## *2.2 Priority Areas in a Watershed*

Numerous studies have indicated that a few areas of the watershed are critical and responsible for high amount of soil erosion and sediment delivery because of differences in environmental attributes across landscapes (Tamene and Vlec, 2007; Tripathi *et al*., 2003). Moreover, as resources for conservation are often limiting, there will be a need to define priorities so that conservation action can be targeted where it is needed most. As a result, identification of priority areas is essential for the effective and efficient implementation of watershed management programmes.

According to UNEP (2003), conservation priorities can be defined in terms of either species or areas. Priority species for conservation are generally those most threatened with extinction, are restricted to small areas (endemics) or have few remaining individuals. Priority areas in a watershed, on the other hand, are those areas that are either sources of priority pollutants in the watershed or are most susceptible to changes that would result in increased input of priority pollutants, resulting in degradation of habitat and water quality (UNEP, 2003). Priority areas in a watershed for conservation measures can be identified by considering physical hazards like drought, soil erosion, sedimentation and excessive percolation under irrigation (Khan *et al*., 2001; Tripathi *et al*., 2003). For instance, a watershed with a higher rate of erosion needs to be given higher priority for soil conservation measures to be adopted.

Priority area identification in a watershed requires considering various factors since watershed is the natural integrator of variables such as precipitation, runoff, erosion and sediment discharge as they relate to input and output in an open hydrological system (Deore, 2005). Keeping this in view, various studies used climatological, pedological, topographic and morphometric parameters to identify and map critical areas, which are proposed as high-priority areas for conservation. For example, Deore, (2005) in his PhD thesis, used multi-criteria analysis to determine priority categories of micro-watersheds in Bhama basin by integrating such factors as slope, erosivity, erodibility, drainage density and elongation ratio. Using concepts of Similar Erosion Risk Potential Units (SERPUs), Lulseged and Vlek, (2005) integrated landscape parameters such as slope, lithology, land use/cover, gully and fraction of surface cover to assess soil erosion and their delivery potential of two catchments of Northern Ethiopia. They also used Transformed Soil Adjusted Vegetation Index (TSAVI) as additional criterion to assess the fractional degree of surface cover and its relative level of degradation. For such input data generation and thereby priority area identification (or micro-watershed prioritization) activities, GIS and RS techniques together with various erosion prediction models have been successfully used in many studies.

## *2.3 Remote Sensing and GIS Application in Watershed Management*

The advancement in the remote sensing and GIS technology provide an effective analytical tool which makes the watershed management relatively simpler.

### 2.3.1 Remote Sensing

Remote sensing has opened a new era in the planning and development of watershed management, as satellites imagery provides a fast and economic way to analyze large watersheds by virtue of their synoptic and repetitive coverage (Jain and Goel, 2002). Thus, by using multispectral data appropriately, different ground features can be differentiated from each other and a thematic map depicting land use can be prepared. Satellite imagery has been well utilized in different studies for watershed characterization and management aims (Saxina *et al.*, 2000) and for measuring qualitative and quantitative terrestrial land-cover changes (Lu *et al.*, 2004a) in a watershed.

For soil erosion assessment in a watershed, remote sensing has been used for both detecting erosion features and obtaining erosion model input data (Petter, 1992; Vrieling, 2006). Satellite data can be applied to directly detect erosion features or to detect erosion consequences. Direct detection has been achieved through identification of individual large erosion features such as gullies. Detectable effects include the damage occurred due to major erosion events, and the sedimentation of reservoirs (Vrieling, 2006).

### 2.3.2 Geographic Information System (GIS)

GIS is characterized by its capability to integrate layers of spatially oriented information. The number and type of applications and analysis that can be performed by GIS in a watershed are as large and diverse as the available geographic datasets (Deore, 2005).

GIS has been widely used in characterization and assessment studies which require a watershed-based approach (Khan *et al*., 2001). In addition, the modeling and visualization capabilities of modern GIS, offer fundamentally new tools to understand the processes and dynamics that shape the physical, biological and chemical environment of watersheds(Jain and Goel, 2002). For example, mapping soil erosion using GIS can easily identify areas that are at potential risk of extensive soil erosion and provide information on the estimated value of soil loss at various locations in the watershed (Shi *et al*., 2004). GIS is thus an important tool for coping with the vast number of spatial data and the relation between data from various sources in the erosion modeling process. As summarized in Saavedera (2005), the advantages of linking soil erosion models with a GIS include: (i) the possibility of rapidly processing input data to simulate different scenarios. A GIS provides an important spatial and analytical function, performing the time consuming georeferencing and spatial overlays to develop the model input data at various spatial scales, (ii) the ability to look at spatial variation; thus areas can be simulated at a user-defined resolution, (iii) the facility of displaying the model outputs (*i.e.*, visualization). Visualization can be used to display and animate a sequence of model output across time and space.

Remote sensing and GIS techniques were utilized in the present study to identity priority areas for conservation measures on the basis of erosion risk.

## *2.4 Spectral Mixture Analysis*

Mixed pixels have been recognized as a problem affecting the effective use of remotely sensed data in Land Use and Land Cover (LULC) classification and change detection. Per-pixel based classification approaches, such as the maximum likelihood classifier (MLC), which are based solely on spectral signatures for LULC classification, often result in poor accuracy (Lu *et al.,* 2004a). The main reasons for this result are the heterogeneity of features on the ground and limited spatial resolution of remotely sensed data such as Landsat TM/ETM (De Asis and Omasa, 2007). Mixed pixels are common in medium spatial resolution remotely sensed data and such pixels have been recognized as a problem for remote sensing applications (Lu *et al.*, 2004b). A mixed pixel is one in which more than one feature is present (e.g. 40% of a pixel might be bare soil, 30% might be Shrub and 30% might be shadow resulting in a complex spectral signature).

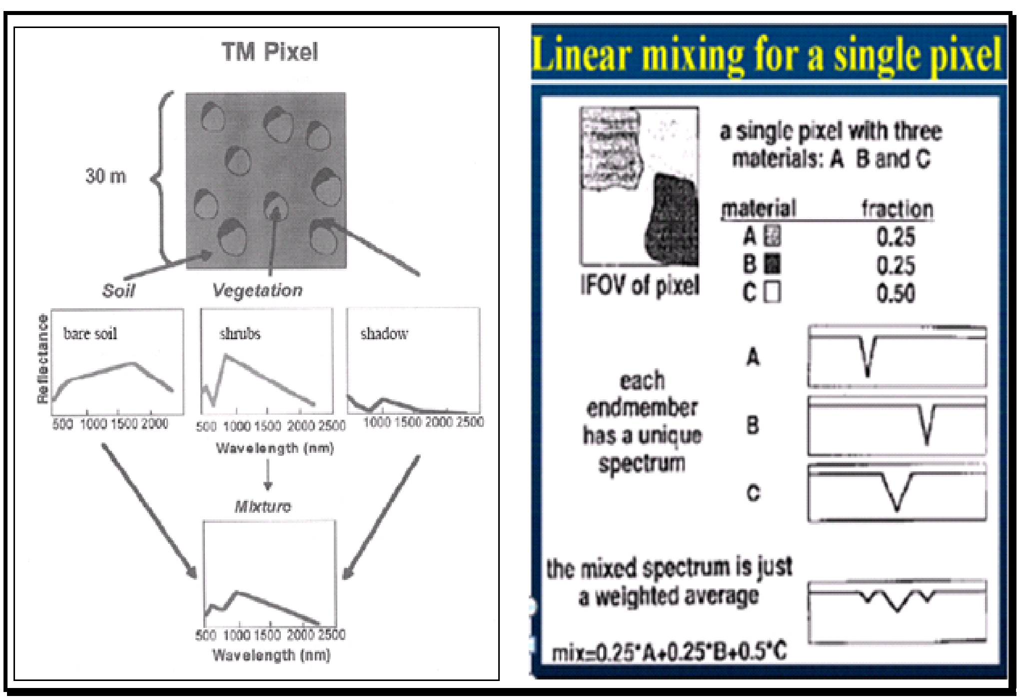


**Figure 2-1 Linear spectral mixture of a single pixel (Roberts *et al.,* 1999; ENVI, 2002)**

Spectral mixture analysis (SMA) has long been recognized as an effective method for ameliorating mixed pixel problems in remote sensing data and it has been proven to be helpful in improving classification accuracy (De Asis *et al.,* 2008, Lu *et al.,* 2003a). The linear spectral mixture analysis model is by far the most common type of SMA, and is widely used because of its simplicity and interpretability. An important assumption of LSMA is that the spectral signature of a given pixel is the linear proportion-weighted combination of the end-member spectra. An end-member is a pure surface material or land cover type that is assumed to have a unique spectral signature (De Asis and Omasa, 2007). The output is typically presented in the form of fraction images for each endmember spectrum, which gives the derived fractions of each endmember spectrum for each pixel. A residual image provides the root mean- square (RMS) of the fit for each (Lu *et al.,* 2003a). The mathematic model of LSMA can be expressed as:

$$R_i = \sum F_j \times R_{Eij} + \varepsilon_i \text{ and } \sum F_j = 1;\ 0 \le F_j \le 1$$

Where i is the number of spectral bands used, j = 1… n (number of end-members), $R_i$ is the spectral reflectance of the mixed pixel in band i, $F_j$ is the fraction of the pixel area covered by the end-member j, $RE_{ij}$ denotes the reflectance of the end-member j in band i, and εi is the residual error in band i.

In remote sensing data applications, as summarized in Lu *et al.,* (2003a), the LSMA approach has been used: 1) to classify vegetation and land-use/land-cover (LULC) classes; 2) to detect LULC changes; 3) to measure sparse vegetation cover; 4) to determine urban vegetation abundance; and 5) to estimate vegetation parameter (RUSLE C-factor) for modeling soil erosion (De Asis and Omasa, 2007).

### 2.4.1 Endmember selection for LSMA

Endmember selection is the most important aspect in SMA. How many endmembers are required for a given study area and how to best identify them are two questions that need to be addressed initially. Regardless of the number of bands, only two to six endmembers are needed to characterize the overall variance in the image (Ustin *et al,.* 1996 as cited in Lu *et al.,* 2004b). In reality, three endmembers (e.g. green vegetation (GV), shade, and soil) and four endmembers (e.g. GV, shade, soil, and non-photosynthetic vegetation (NPV)) are often used on TM image (Adams *et al.,* 1995; De Asis and Omasa, 2007).

For many applications of SMA using remote sensing data, image endmembers are often used because they can be easily obtained and they represent the spectra measured at the same scale as the image data (Lu *et al.,* 2004b). Image endmembers are derived from the extremes of the image feature space, assumed to represent the purest pixels in the images. However, if an image does not contain sufficiently pure examples of a specific material to allow its identification from the spectra of individual pixels, then it is necessary to use reference endmembers to link image endmembers with actual target materials (Adams *et al.*, 1995). Selecting reference endmembers from a spectral library or from field measurements is often flexible, but it is difficult to account for all possible features and processes due to different factors influencing the data spectra from spectral library information. Selection of endmembers is often an iterative process (Lu *et al.,* 2004b). Evaluating the fraction images and residual images are prerequisite to refining endmembers. The characteristics of a study area and its scale are also important factors affecting the decision of endmember selection. An ideal endmember selection method should be easy to implement and to identify the true endmembers (Lu *et al.*, 2004b).

## *2.5 Soil Erosion*

### 2.5.1 Soil Erosion Extent

Soil erosion is one of the most serious environmental problems in the world today, as it threatens agricultural and natural environment (vrieling, 2006). According to sources cited in (Deore, 2005), study on global soil loss has indicated that soil loss rate in the U.S. is 16 t/ha/yr; in Europe it ranges between 10 – 20 t/ha/yr, while in Asia, Africa and South America between 20 and 40 tons/ha/yr.

The recorded annual soil erosion in Ethiopia ranges from 16-300 tons/ha/yr depending mainly on the slope, land cover, and rainfall intensities (Hawando, 1995). According to the Ethiopian highland reclamation study (FAO 1984), in mid 1980's 27 million ha or almost 50% of the highland area was significantly eroded, 14 million ha seriously eroded and over 2 million ha beyond reclamation. Soil loss by erosion from 6 SCRP sites in various parts of Ethiopia ranges from 18–214.8 tons/ha/yr (Table 2-1).

**Table 2-1 Soil erosion loss on six SCRP sites (Wolde Aragaye Berehe, 1996)**

| *Sites* | *South Wollo* | *Sidamo* | *Harar* | *North Showa* | *Gojam* | *Illubabur* |
|---|---|---|---|---|---|---|
| **Soil loss t/ha/yr** | 36.5-53.8 | 41.2-49.5 | 25.5-27.8 | 152.4-214.8 | 40.2-199..2 | 18.0-135..3 |

### 2.5.2 Soil Erosion Types

Soil erosion is the removal of soil from a landscape by erosive agents such as water and wind. Water erosion involves the detachment, transport and deposition of soil particles by the erosive forces (Renard *et al*., 1997). Soil erosion occurs in various forms (*e.g.,* splash, sheet, rill, gullies) depending on the stage of progress in the erosion cycle and the position in the landscape.

#### *2.5.2.1 Rain splash Erosion*

Rain splash Erosion is the result of water falling directly on to the ground during rainstorms or when it is intercepted by the canopy and finds its way through the ground (Morgan, 1995). Some of the water infiltrates into the soil, while some water stays on the surface saturating it and weakening natural soil aggregates so that the impact of subsequent raindrops breaks them down.

#### *2.5.2.2 Sheet Erosion*

Sheet erosion is movement of soil from raindrop splash resulting in the breakdown of soil surface structure and surface runoff; it occurs rather uniformly over the slope and may go unnoticed until most of the productive topsoil has been lost.

#### *2.5.2.3 Rill Erosion*

Rill initiated at a critical distance down slope where surface runoff concentrates and becomes channeled. These channels are called rills when they are small enough to not interfere with field machinery operations. The water in a rill has sufficient depth for turbulence to develop in it and therefore entrain large particles (Morgan, 1995).

#### *2.5.2.4 Gully Erosion*

Gully erosion is defined as the erosion process whereby runoff water accumulates and often recurs in narrow channels and, over short periods, removes the soil from this narrow area to considerable depths (Poesen *et al.,* 2003). Gullies can be either permanent or ephemeral. Permanent gullies are often defined for agricultural land in terms of channels too deep to easily ameliorate with ordinary farm tillage equipment, typically ranging from 0.5 to as much as 25–30 m depth (Poesen *et al.,* 1996). In concept, ephemeral gullies are easily defined as the "missing link" between rills and permanent waterways (Thorne *et al.,* 1986). Ephemeral gullies are small channels eroded by concentrated overland flow that can be easily filled by normal tillage, only to reform again in the same location by additional runoff events (Poesen *et al.,* 2003). Runoff becomes concentrated in low points, or swales, where flow lines converge from neighboring high points, or spurs. As concentrated surface runoff is found mostly in swales, it is to be expected that ephemeral gullies that form due to concentrated flow erosion should be found there also (Thorne *et al*., 1986).

Gully systems in Ethiopia can often be considered as discontinues ephemeral streams (Bull, 1997 as cited in Nyssen, 2001). Assessments of gully erosion volumes in Ethiopia are rare. Using photogrammetric techniques, Shibru *et al*., (2003) estimate that between 1966 and 1996, 700,000 tons of soil were lost by gully erosion from a 9-km$^2$ catchment in the eastern highlands (26t/ha/yr). Using monitoring and interview techniques to establish average long-term soil loss rates by gully erosion in Central Tigray, Nyssen (2001) obtained 5t/ha/yr.

Most soil erosion models do not predict the location of gullies. An approach to predict locations where gully heads might develop is presented by the threshold concept (Poesen *et al*., 2003). In order to predict the potential location and spatial patterns of gullies in the study area, the method proposed by Thorne *et al.,* (1986) and Moore *et al,*. (1988) were used.

### 2.5.3 Factors of Soil Erosion

Soil erosion and transport is a complex process that is influenced by climate, soil type, topography, and land use.

#### *2.5.3.1 Climatic factors*

Soil erosion occurs when raindrops act upon the soil particles. Soil loss is closely related to rainfall partly through the detaching power of raindrops striking the soil surface and partly through the contribution of rain to runoff. Potential ability of rain to cause erosion is known as erosivity (R) factor (Renard *et al*., 1997). Raindrops while falling acquire kinetic energy and on impact, the kinetic energy is used up in detaching the soil particles. Energy is required to break the soil aggregates, splashing them and subsequently carrying them with runoff (Saavedra, 2005).

#### *2.5.3.2 Soil Factor*

The susceptibility of soil to erosion agents is generally referred to as soil erodibility (Renard *et al*., 1997). Soils differ in their resistance to erosion, which is a function of a range of soil properties such as texture, structure, soil moisture, roughness, and organic matter content (Deore, 2005).

Generally, soils with faster infiltration rates, higher levels of organic matter and improved soil structure have a greater resistance to erosion. Soils high in clay have low K values, because they are resistant to detachment. Coarse textured soils, such as sandy soils also have low k values, because of low runoff even though these soils are easily detachable. Medium textured soils, such as silty loam soils, have a moderate k values, because they are moderately susceptible to detachment and they produce moderate runoff. Soils having high silt content are the most erodible of all soils as they cause a decrease in infiltration (Saavedra, 2005).

#### *2.5.3.3 Topographic Factors*

The slope factors (LS) refer to topographic and/or relief factor. Erosion would normally be expected to increase with increase in slope steepness and slope length as a result of respective increases in velocity and volume of surface runoff (Doere, 2005). However, soil loss is much less sensitive to changes in slope length than to changes in slope steepness (McCool *et al.*, 1987 as cited in Remortel *et al*., 2001). Steeper terrain slopes cause higher runoff velocities, more splashes downhill and faster flow and therefore contributes greater soil erosion. Erosion only doubled for a steepness change from 2-20% and the erosion rate tends to level off (Remortel *et al*., 2001). A slight increase in detachment rate probably occurs as the raindrops strike at a greater angle, but this effect should not cause a major change in total splash detachment.

#### *2.5.3.4 Ground Cover Factor*

Vegetation cover is one of the most crucial factors in reducing soil erosion. Vegetation reduces soil erosion by: protecting the soil against the action of falling raindrops, increasing the degree of infiltration of water into the soil, reducing the speed of the surface runoff, binding the soil mechanically, maintaining the roughness of the soil surface, and improving the physical; chemical and biological properties of the soil (De Asis and Omasa, 2007).

Differences in erosion rates are commonly related to land use in areas where soil, climate, and topography are similar, For example, in Malaysia, the rate of soil erosion increased from 0.24 ton/ha/yr under natural forest to 4.9 ton/ha/yr in areas of mature coffee, to 7.32 ton/ha/yr in areas with cultivated vegetable crops (Lal, 1990 as cited in López, 1998). In Puerto Rico, soil erosion in coffee plantations without ground cover was ten times greater than from adjacent areas of coffee with natural ground cover (Smith and Abruña, 1955 as cited in López, 1998). To account for the effect of vegetation in erosion assessments, a cover and management factor (C-factor) has often been used. The C-factor is defined as the ratio of soil loss from land cropped under specified conditions to the corresponding clean-tilled continuous fallow (Wischmeier and Smith, 1978).

For deriving and mapping ground cover factor or C factor, various approaches have been used. Traditionally, spatial estimates of vegetation cover, or C factor, have been done by simply assigning C factor values from literature or field data into a classified land cover map (Folly *et al.,* 1996). This method, however, resulted in C factor estimates that are constant for relatively large areas, and do not adequately reflect the variation in vegetation that exists within large geographic areas. Normalized Difference Vegetation Index (NDVI) has also been explored for mapping the C factor (De Jong, 1994 in De Asis and Omasa 2007). Result in De Asis and Omasa (2007) proved that LSMA-derived C factors produced a more detailed spatial variability, as well as generated more accurate erosion estimates when used as input to RUSLE model. Therefore, this study used SMA method to derive C factor

#### *2.5.3.5 Conservation Practice Factor*

Especially in agricultural areas, conservation practices such as contouring, strip cropping, or terracing, reduce soil losses. For instance, in areas where there is terracing, runoff speed could be reduced with increased infiltration, ultimately resulting in lower soil loss and sediment delivery. The effectiveness of such practices is often analyzed with a support practice factor (P-factor) which is defined as the ratio of soil loss with the practice applied and up- and downslope cultivation (Wischmeier and Smith, 1978; Renard *et al*., 1997). P-values have been assigned to land use classes using literature values and ranges from 0 to 1 (Kaltenrieder, 2007).

### 2.5.4 Soil Erosion Models

The difficulty in observing and measuring erosion processes during runoff or erosion events, owing to the small spatial and time scales at which the processes occur, necessitates the use of erosion models for the prediction of erosion and sedimentation in catchments (Jetten *et al.,* 2003 cited in Saavedra, 2005 ). Erosion models allow users to ascertain temporal trends, examine spatial variations, identify critical processes and explore the possible impacts of remedial measures and the relative effectiveness of implementations strategies for erosion and sedimentation controls (Baigorria and Romero, 2007). Modeling in soil erosion is the process of mathematically describing soil particle detachment, transport and deposition on land surfaces. The objective of soil erosion models is either predictability or explanatory (Petter, 1992). In general, the models fall into three main categories: conceptual, empirical and physically based models.

***Conceptual models*** lie somewhere between empirical and physically based models, and aim at reflecting the physical processes governing the system but describe them with empirical relationships (Deore, 2005). Conceptual models tend to include a general description of catchment processes, without including the specific details occurring in the complex process interactions. Because parameter values are determined through calibration against observed data, conceptual models tend to suffer from problems associated with the identification of the parameter values (Saavedra, 2005).

***Physically based models*** are based on an understanding of the physics of the erosion and sediment transport processes (Deore, 2005). In principle, they can be applied outside the range of conditions used for calibration and, as their parameters have a physical meaning, they can be evaluated from direct measurements and without the need for long hydro-meteorological records (Saavedra, 2005). Examples of physically based models are the Morgan-Morganand Finney (MMF), Water Erosion Prediction Project (WEPP) and the Soil and Water Assessment Tool (SWAT).

***Empirical models*** are generally the simplest of the three model types. They are based primarily on defining important factors through field observation, measurement, experimentation and statistical techniques relating erosion factors to soil loss (Petter, 1992). The computational and data requirements for such models are usually less than for conceptual and physically based models (Li *et al*., 1996). They are particularly useful as a first step in identifying the sources of sediments. The Universal Soil Loss Equation (USLE) and its revised version RUSLE are two of the empirical models that have been most widely used and generally accepted by the natural resources community because they are relatively easy to use (Saavedra, 2005).

In this study RUSLE was chosen over other methods because of its ease of implementation, reliance on easily accessible data and its relatively accurate results.

### 2.5.5 RUSLE Model

The Revised Universal Soil Loss Equation (RUSLE) is an empirically based model that has the ability to predict the long term average annual rate of soil erosion on a field slope as a result of rainfall pattern, soil type, topography, crop system and management practices (Renard *et al.,* 1997). It retains the factors of the USLE by including improved means of computing soil erosion factors. The RUSLE model in GIS environment can predict erosion potential on a cell-by-cell basis, which is effective when attempting to identify the spatial pattern of soil loss present within a large watershed area (Shi *et al.,* 2004). GIS can then be used to isolate and query these locations to identify the role of individual variables in contributing to the observed erosion potential value (Saavedra, 2005). In spite of this advantage, RUSLE does not estimate remote deposition and gully erosion.

RUSLE computes average annual erosion as (Renard *et al.,* 1997):

$$\mathbf{A = R * K * L * S * C * P}$$

Where: A = computed average annual soil loss in tons/acre/year; R = rainfall-runoff erosivity factor; K = soil erodibility factor; L = slope length factor S = slope steepness factor; C = cover management factor; and P = conservation practice factor.

### 2.5.6 On-site versus off-site effects of soil erosion

Effects of soil erosion, impact on actual and potential productivity, are complex and governed by numerous interacting factors. In general the effects can be either on-site or off-site effects. In Ethiopia, the on-site impacts of soil erosion are most frequently studied, typically by estimating the productivity losses as economic cost of soil erosion. Less well known and documented are the off-site costs of soil erosion (Eyasu, 2003).

#### *2.5.6.1 On-site effects*

On-site effects are those that happen at the site where erosion occurs. These effects include two consequences of accelerated erosion: (i) short/immediate or direct effects on plant growth and (ii) long-term/potential or indirect effects due to adverse changes in soil quality (Lal, 1998). The immediate or direct impacts usually involve damage to the crop on the ground. The long-term effects involve changes to soil quality that impact growth and productivity of crops to be grown in the future (Figure 2-2). In Ethiopia, the EHRS estimated an on-site productivity loss of 60 million Ethiopian Birr in 1986 due to soil erosion (FAO, 1986; Sutcliff, 1993).

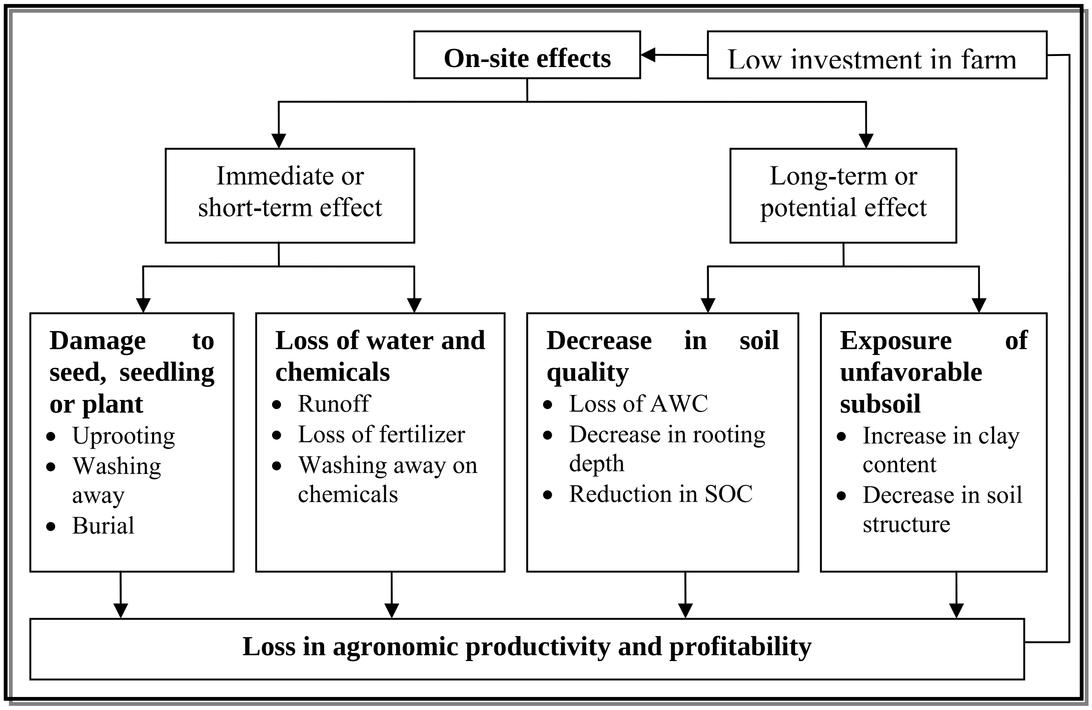


**Figure 2-2 on site effects of soil erosion (Lal, 1998)**

#### *2.5.6.2 Off-site effects*

Off-site effects are those that occur when runoff and sediments from one field, watershed or waterway enter another. Siltation of water reservoirs has a considerable impact on the reservoir functions by reducing their storage capacity (Eyasu, 2003; Tamene and Vlek 2007). According to Shahin (2001) cited in Nyssen, (2001), yearly $18x10^6$ tons of sediments would enter into Koka reservoir from its approximately 4050 $km^2$ catchment. Lal (1998) classified the off-site effects of soil erosion into three categories: (i) damage to present and future crop growth, (ii) adverse change in environment; and (iii) damage to civil structure (Figure 2-3).

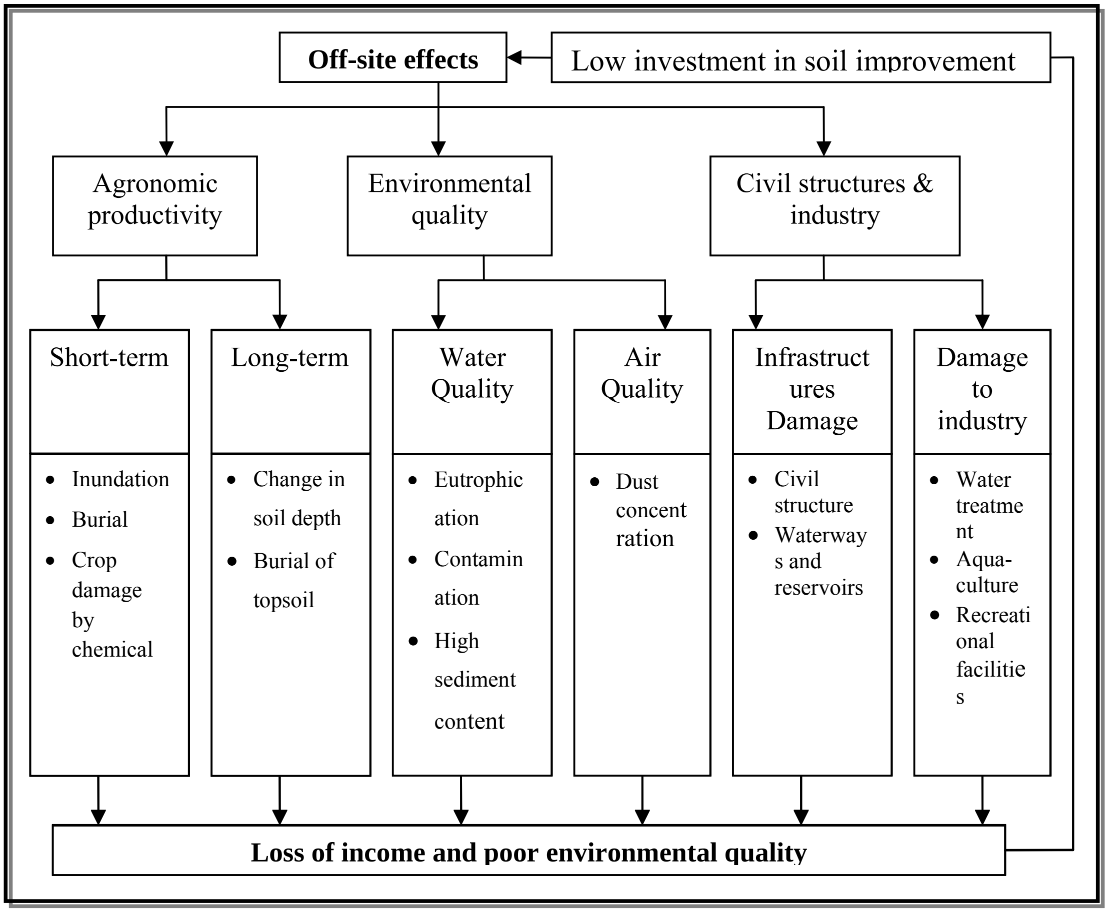


**Figure 2-3 Off site effects of soil erosion (Lal, 1998)**

### 2.5.7 Erosion and siltation problem in the study area

Estimates for soil erosion based on the sediment curve at Mojo gauging station and on an average sedimentation rating in Koka reservoir are an order of magnitude higher at 15-25 ton/ha/yr (MoWR, 2008). The fundamental causes of soil erosion in the study area are the severe impact of human activities (i.e. cultivation and grazing) on natural resources. This is due the rapid increase in human and livestock population which is greater than the carrying capacity of the natural resource. This has resulted in fast spread of gullies and an irreversible degradation of natural resource (MoWR, 2008).

Soil erosion in turn causes serious downstream negative multiple effects with high social and economical effects. The Metallitia earth dam near the Modjo River, for instance, filled with 96000 $m^3$ of sediments in two years, largerly due to sediments from intense gullies (PRDE, 1989). Sedimentation of Koka reservoir has also been an ongoing problem since its impoundments. According to Eyasu (2003) estimates, Koka dam has lost about 30% of its designed storage capacity due to siltation. Among other effects, the currently enacted power rationing of power supply to towns is the function of the level of depletion of the storage of the dam below the level required to fully satisfy the expected demands. Other impacts of the reduction of the active storage volume of dam are loss of reservoir capacity to regulate water supply to irrigation and flood control services for downstream towns.

## *2.6 Multi-Criteria Decision Analysis*

Decision Analysis is a set of systematic procedures for analyzing complex decision problems (Eastman, 2006). These procedures include dividing the decision problems into smaller more understandable parts; analyzing each part; and integrating the parts in a logical manner to produce a meaningful solution (Malczewski, 1999).

To meet a specific objective, it is frequently the case that several criteria will need to be evaluated. Such a procedure is called *Multi-Criteria Evaluation* (Eastman, 2006). MCDA techniques can be used to identify a single most preferred option, to rank options, to list a limited number of options for subsequent detailed evaluation, or to distinguish acceptable from unacceptable possibilities (Malczewski, 2004). For example, areas of concern for soil erosion can be identified on the basis of such criteria like slope, landuse, soil type, etc.

### 2.6.1 Multi-criteria Decision Analysis (MCDA) in GIS

Any spatial decision problem can be structured into three major phases (1) intelligence phase which examines the existence of a problem or the opportunity for change, (2) design phase which determines the alternatives and (3) choice phase which decides the best alternative (Simon, 1960 as cited in Malczewski, 1999). Increasingly, GIS capabilities for data storage, management, manipulation and analysis are used as an important aid for spatial decision making in all these stages. As clearly discussed in Malczewski, (1999), the integration of MCDM techniques with GIS has considerably advanced the conventional map overlay approaches in environmental management. GIS-based MCDA efficiently combines and transforms spatial (geographic) and aspatial (attribute) data into a resultant decision (output). Since spatial multi-criteria analysis includes an explicit geographic component, it is vastly different from conventional MCDA techniques it (Malczewski, 2004).

### 2.6.2 Multi-criteria Decision rules

According to Eastman, (2006) definition, a decision rule is a procedure by which criteria are selected and combined to arrive at a particular evaluation, and by which evaluations are compared. A decision rule might be as simple as a threshold applied to a single criteria (such as, all regions with slopes less than 35% will be zoned as suitable for development) or it may be as complex as one involving the comparisons of several multi-criteria evaluations (Eastman, 2006).

Broadly, the decision rules can be classified into multi-objective and multi-attribute decision making methods (Jankowski 1995). The multi-objective approaches are mathematical programming model oriented methods, while multi-attribute decision making methods are data oriented. Due to computation complexity, multi-objective optimization methods are difficult to implement in the GIS environment. The multi-attribute (or multi-criteria) approaches are much easier to implement in GIS especially in the raster data model (Malczewski, 2004). This approach includes various evaluation methods including Weighted Linear Combination (WLC) and its variants, Ordered Weighted Averaging (OWA), analytic hierarchy process (AHP).

**Analytical Hierarchy Process** (AHP) is an excellent and well-known weight evaluation method (Malczewski, 2004). This method is based on three principles: decomposition, comparative judgment and synthesis of priorities. In the first step of AHP, complex decision problem is decomposed into simpler decision problems to form a decision hierarchy. Once decomposition is completed, an expert would be asked to make pairwise comparisons between two factors at a time to decide which factor is more important. The final step is to combine the relative weights of the levels obtained in the previous step to produce composite weights (Jankowski 1995).

# 3 METHODOLOGY

## 3.1 Description of the Study Area

### 3.1.1 Location and Accessibility

The study area is found in the main Ethiopian rift extending up to the eastern escarpment. It is part of the upper Awash River basin and covers partially Lumie, Addaa chuluka and Gimbichu weredas in Eastern showa zone of Oromia regional state. However, the vast majority of the study area is found in Lomie and addaa chuluka weredas. Geographically the study area lies between $38^0 54'22''$ to $39^0 17'18''$E and $08^0 24'15''$ to $09^0 07'49''$N. The watershed covers surficial area of 1645.77 $km^2$. The surrounding area is accessible by all weather road and seasonal gravel roads (Figure 3-1).

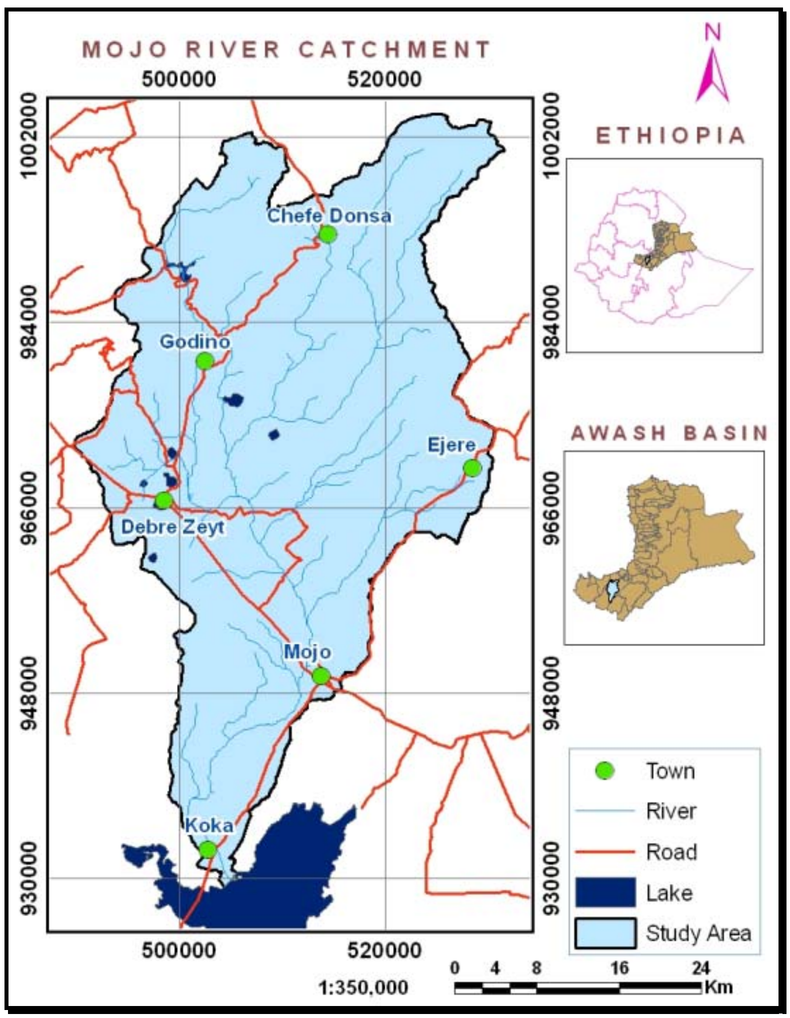


**Figure 3-1 Location of the Study Area**

### 3.1.2 Climate

The climate of the study area comes under the influence of the ITCZ and the seasonal rainfall distribution results from the annual migration of the ITCZ. Twenty years rainfall records for 6 stations within and adjacent to the study area show an average annual rainfall between 780.9mm and 981.2mm with a mean annual value of 887.3.mm. Most rainfall occurs between June and September. Although the rainfall is bimodal, the short rains (Belg) are erratic and not sufficient for rain fed crops (Eyasu, 2003). The annual temperature of the study area is 19.5$^0$c with average winter high of 24.1$^0$c in May at Koka dam and an average low of 14.8$^0$c in December at Chefedonsa. Table 3-1 and 3-2 shows average monthly rainfall and temperature obtained from National Meteorological Stations of Ethiopia that covers 20 years (1986-2005).

**Table 3-1 Average monthly rainfall in mm of six stations (1986-2005)**

| Station | Jan | Feb | Mar | Apr | May | Jun | Jul | Aug | Sep | Oct | Nov | Dec |
|---|---|---|---|---|---|---|---|---|---|---|---|---|
| Koka dam | 12.3 | 28.6 | 58.7 | 74.7 | 43.5 | 80.9 | 215 | 263 | 83.1 | 30.6 | 3.6 | 5 |
| Mojo | 11.4 | 23.6 | 58.7 | 54.2 | 53 | 104 | 255 | 216 | 105 | 29.4 | 7.2 | 2.2 |
| Debre Zeit | 10.4 | 14.7 | 56.7 | 53 | 37.3 | 99.3 | 192 | 195 | 90.8 | 23.4 | 4.2 | 4.4 |
| Ejere | 15.2 | 35.4 | 47.9 | 50.5 | 42.7 | 76.6 | 209 | 236 | 101 | 28.8 | 7.8 | 7.7 |
| Chefedonsa | 9.3 | 36.3 | 53.2 | 62.9 | 40.8 | 99.7 | 196 | 249 | 114 | 15.5 | 2.7 | 5.3 |
| Akaki | 10.9 | 32.1 | 57.7 | 90.5 | 61.9 | 111 | 236 | 240 | 109 | 24.4 | 3.3 | 4.1 |

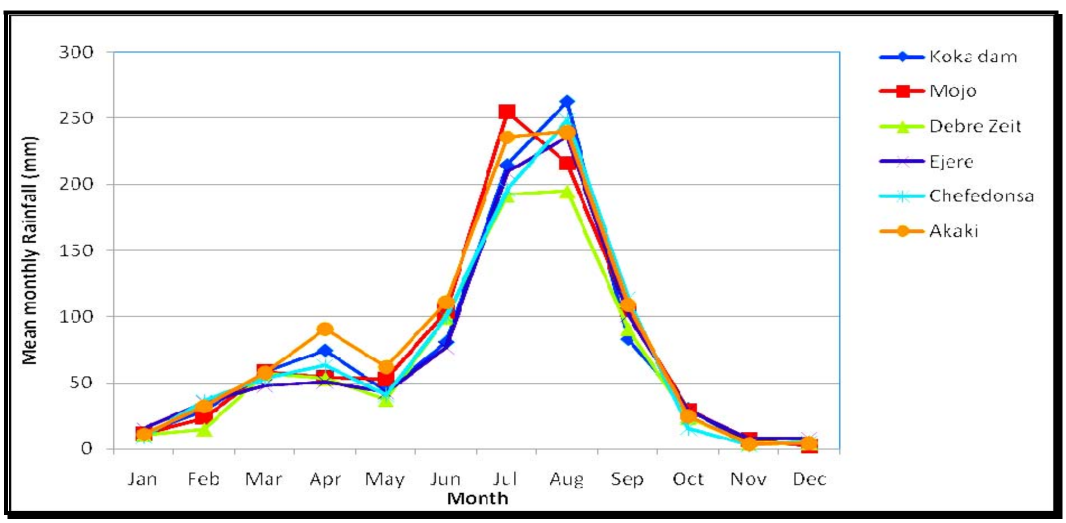


**Figure 3-2 Average Monthly Rainfall of Six Stations (1986-2005)**

**Table 3-2 Average Monthly temperature ($^0$c) values of four stations (1986-2005)**

| Station | | Jan | Feb | Mar | Apr | May | Jun | Jul | Aug | Sep | Oct | Nov | Dec |
|---|---|---|---|---|---|---|---|---|---|---|---|---|---|
| Koka Dam | Max | 30.2 | 31.7 | 32.5 | 30.9 | 33.1 | 31.3 | 30.3 | 31.1 | 31.9 | 29 | 29.2 | 29.6 |
| | Min | 12.9 | 14.5 | 15 | 14.3 | 15.1 | 14.1 | 14 | 14.2 | 14.2 | 11.6 | 12.3 | 12.3 |
| | **Mean** | **21.6** | **23.1** | **23.7** | **22.6** | **24.1** | **22.7** | **22.1** | **22.6** | **23.1** | **20.3** | **20.8** | **20.9** |
| Mojo | Max | 28.9 | 29.8 | 29.8 | 30.8 | 31.5 | 29.9 | 26.9 | 27.5 | 28.9 | 29.6 | 29.3 | 28.1 |
| | Min | 8.88 | 9.78 | 11.2 | 12.3 | 12.7 | 9.74 | 10 | 10.2 | 10.1 | 9.0 | 8.58 | 6.68 |
| | **Mean** | **18.9** | **19.8** | **20.5** | **21.6** | **22.1** | **19.8** | **18.5** | **18.9** | **19.5** | **19.3** | **19.0** | **17.4** |
| Debre Zeit | Max | 26.7 | 29.2 | 28.3 | 28.5 | 29.3 | 27.5 | 24.6 | 24.4 | 25.9 | 26.9 | 25.9 | 25.9 |
| | Min | 10.5 | 11.4 | 12.9 | 13.5 | 13 | 13.1 | 13.7 | 13.9 | 12.8 | 10.4 | 9.34 | 8.98 |
| | **Mean** | **18.6** | **20.3** | **20.6** | **21** | **21.2** | **20.3** | **19.1** | **19.2** | **19.3** | **18.6** | **17.6** | **17.4** |
| Chefe-Donsa | Max | 21.7 | 23.7 | 23.4 | 23.7 | 25 | 23.4 | 21.1 | 21.1 | 21.7 | 22.2 | 21.7 | 21.2 |
| | Min | 9.26 | 10.1 | 11.7 | 12.3 | 12.1 | 11.3 | 11 | 11.4 | 11.5 | 10.2 | 8.4 | 8.5 |
| | **Mean** | **15.5** | **16.9** | **17.6** | **18** | **18.6** | **17.3** | **16.1** | **16.3** | **16.6** | **16.2** | **15.0** | **14.8** |

### 3.1.3 Topography

The topography of the study area is generally characterized by gently undulating terrain. Of the total area, 48.1 % (791 km$^2$) lies within the slope range of 0-10 % which is generally flat to gently undulating topographic feature (Table 3-3). Elevations of the watershed vary from 1590 m to 3062 m above mean sea level (Figure 3-3).

**Table 3-3 Slope range of the study area**

| SLOPE (%) | CLASS NAME | AREA | | |
|---|---|---|---|---|
| | | ha | Km$^2$ | Percentage |
| **0 - 2** | Flat to almost flat terrain | 56977.7 | 569.8 | 34.6 |
| **2 - 10** | Gently flat to undulating terrain | 79096.1 | 791.0 | 48.1 |
| **10 - 15** | Rolling terrain | 13195.6 | 132.0 | 8.0 |
| **15 - 30** | Hilly terrain | 10906.6 | 109.1 | 6.6 |
| **>30** | Steep dissected to mountainous terrain | 4390.6 | 43.9 | 2.7 |
| **Total Area** | | **164566.6** | **1645.7** | **100** |

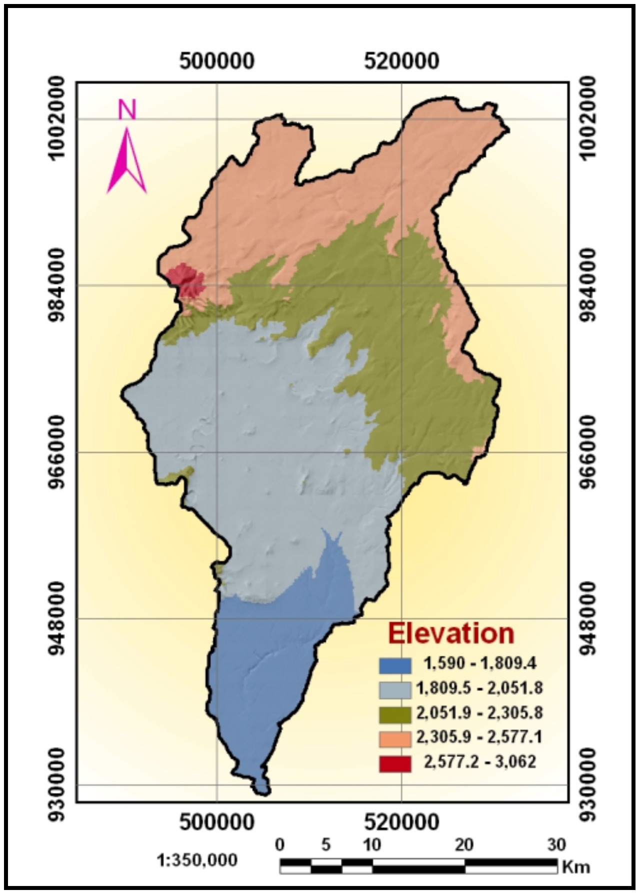


**Figure 3-3 Topography of the Study Area**

### 3.1.4 Vegetation

Much of natural vegetation in the area has been destroyed or altered by prolonged cultivation and human settlements. Before the 1950s, the report by FFDME (2001) and the elders of the area indicate that, the mountainous areas were covered with indigenous trees of mainly *Juniperus procera*. Other common bush and shrub species include *Dodonea angustifolia, Carissa edulis, Otostegia integrifolia, Rhus retinorrhoea, Osyris compressa, Myrsine africana*, *Euclea shimperi*, *Erica arborea* and others. In addition to these species, the common tree species currently found in the watersheds include, , *Eucalyptus camaldulensis and Euphorbia* spp. (around homes), *Acacia albida, A. seyal, A. sieberiana* (on farm lands). *Eucalyptus camaldulensis,* which was introduced to the area in 1950s (FFDME, 2001) seems to increase in the landscape.

### 3.1.5 Soil and Geology

Vertisols are the major soil types accounting for about 86.1% of the total land mass of the area. The two dominant vertisols in the watershed are pellic vertisols (41.8%) and vertic cambisols (42.3%). Other soil types of minor importance are Luvic phaeozems which cover about 9.5% of the land mass. Chromic luvisols and eutric fluvisols covers 5.6% and 0.7% of the study area respectively. Vertislos are good chemical fertility but they have physical limitation for crop production. Phaeozems are well drained but they are shallow soils with low fertility and poorly developed structure (aggregate). These soils are very prone to water erosion. This partly explains the high rate of soil erosion in the watershed area. As to the geological set up, the area belongs to the Quaternary rocks of Pleistocene and Holocene, which is not yet differentiated to certain rock groups, and tertiary basalt of Paleocene-Oligocene-Miocene age of the plateaus adjoining to the rift.

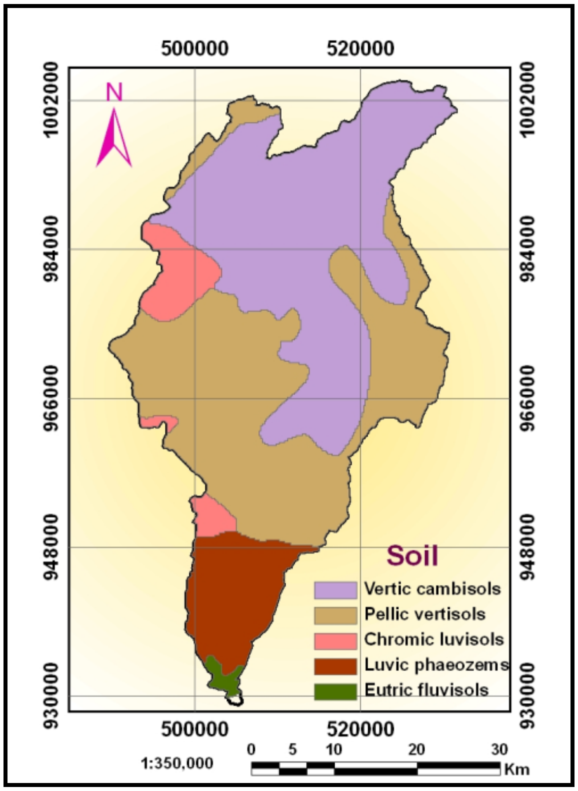


**Figure 3-4 Soil map**

### 3.1.6 Gully Erosion

Due to the topography and possibly poor vegetative cover in the study area, flash flood is released forcefully down to the productive bottomlands. When the floods reach the bottomlands (Vertisols), the soft and easy to move soils are easily damaged. As a result of poor farmers' management practices, easy movement of the soils is facilitated and thus gully erosion enhanced. It is very common to see the highly productive lands affected by gullies. In addition to damaging the productive lands and affecting productivity, accessibility is affected during the rainy seasons and many farmers complain about this issue. During rainy seasons, large amount of water is carried down the slope resulting in flash floods. These are causing enormous damage on the existing trails through the change of courses, silt deposition, increasing in width, depth and number of these gullies.

**Figure 3-5: Gully erosion in the study area**

### 3.1.7 Drainage

The Mojo River and its tributaries are perennial source of water in the study area. However, this river is highly polluted due to discharge of chemicals from the various industrial plants located along the river banks. The Mojo River drains the area flowing southward and finally entering into the Koka reservoir. Other major surface water in the watershed includes Koka reservoir, Bishoftu, Hora, kuriftu lakes.

### 3.1.8 Population

According to the 2007 Population and Housing Census, the population of three weredas covering the study area was 434,126. Most of the population (66.6%) centers are in the rural areas and the remaining (33.4%) centers are in the rural areas (Table 3-4). The rapidly expanding population in the area is placing increasing pressure on agricultural land and forests resulting in overgrazing, deforestation and land degradation.

**Table 3-4: Population of weredas covering the study area**

| No | Wereda | Urban | | | Rural | | | Urban + Rural | | |
|---|---|---|---|---|---|---|---|---|---|---|
| | | Male | Female | Both Sexes | Male | Female | Both Sexes | Male | Female | Both Sexes |
| 1 | Lome | 18937 | 19805 | 38742 | 40899 | 36860 | 77759 | 59836 | 56665 | 116501 |
| 2 | Gimbichu | 3021 | 3306 | 6327 | 41771 | 38140 | 79911 | 44792 | 41446 | 86238 |
| 3 | Ada-a | 47938 | 52176 | 100114 | 68381 | 62892 | 131273 | 116319 | 115068 | 231387 |
| | **Total** | **69896** | **75287** | **145183** | **151051** | **137892** | **288943** | **220947** | **213179** | **434126** |

## 3.2 Data sources and Methods

### 3.2.1 Data Acquisition

#### *3.2.1.1 Data Acquisition*

To achieve the objectives outlined in the section 1.2, the following relevant information was collected / generated from various sources.

- ***Satellite Data***

Cloud free and 2005ETM+ scene covering the study area was selected for analysis. The utility of Landsat imagery for studying watershed erosion has long been suggested as a time and cost-efficient method.

**Table 3-5 Main characteristics of the imagery used in the study area**

| Sensor | Acquisition Date | Path/Row | Spatial Resolution | Spectral Resolution | Temporal Resolution |
|---|---|---|---|---|---|
| Thematic Mapped (ETM+) | 3 Dec 2005 | 168/54 | 30m*30m | 8 bit | 16 days |

- ***Field Data***

Field work was carried out during the dry season in March 2010. Prior to the fieldwork, a detailed examination of False Color Composite of a Landsat ETM image and a topographic map of the study area was conducted to get an overall view and to systematically identify and select sampling areas depending on the accessibility of each site. A GPS was used to locate and define the sampling areas. Meanwhile, Information was collected about physical aspects of vegetation cover and erosion features in the area.

***Ancillary data***

Ancillary data were collected from different reports and departments in the study area. Topographic data (DEM) and soil data were collected from Ministry of Water Resource and Geological Survey of Ethiopia and used in the analysis and interpretation of the results. Climatic data such as annual rainfall from (1986-2005) were also gathered from National Meteorological Agency and well adopted for the analysis. The study tried to use the optimum availability of ancillary data to achieve the objectives of the study.

### 3.2.2 Methods

#### *3.2.2.1 Micro-watershed Delineation*

With the widespread availability of digital elevation databases, watershed delineation has been automated in many GIS/hydrologic software. The watersheds under study were delineated using the automatic delineation option available in ArcHydro Tools 9.1 Extension. Patched DEM derived from SRTM data was used in the delineation procedures. Any areas of internal drainage are filled in so as to create depression less elevation grid. From filled DEM, flow direction then flow accumulation was generated. Based on an iterative process to find the best stream threshold value, 33 micro-watersheds were delineated (Figure 3-6). Area of the micro-watersheds ranges between 15.4 km$^2$ (MW25) and 132.2 km$^2$ (MW4).

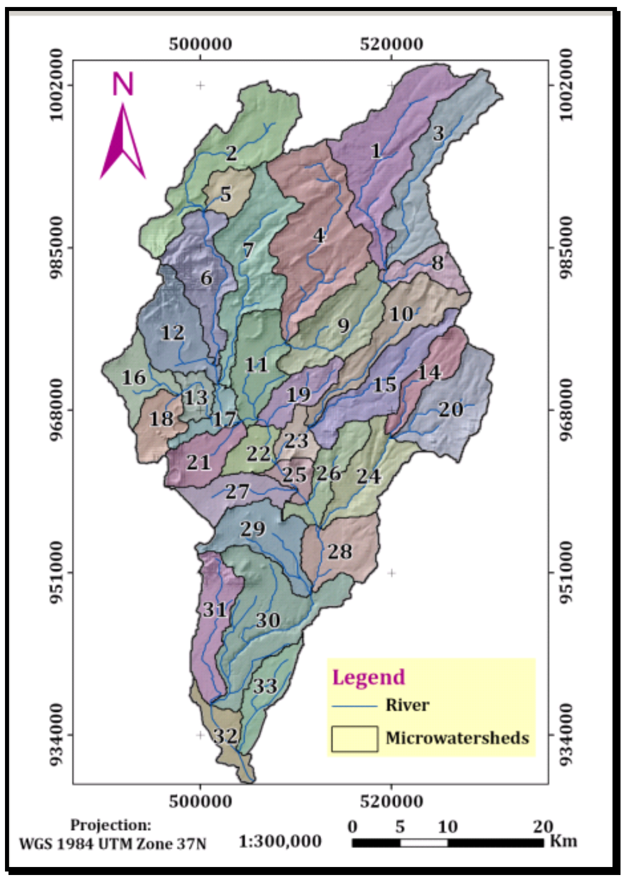


**Figure 3-6 Map of micro-watersheds**

#### *3.2.2.2 Micro-watershed prioritization*

Two approaches were adopted for identification of priority areas in Mojo River Watershed based on soil erosion-proneness of micro-watersheds: Revised Universal Soil Loss Equation and Multi-Criteria Analysis. The RUSLE model developed by Renard *et al.*, (1997) was used in this study for estimation of soil loss. To perform MCA, criteria (slope, gully location, landcover and soil type) have been derived from various sources. Digital Elevation Model (DEM) from the SRTM data has been used to obtain slope and potential gully location of the micro-watersheds. Landuse/landcover map has been produced from satellite data using Maximum likelihood classification. Input parameters for RUSLE model and MCA approach were derived through GIS analysis and digital image processing.

GIS analysis included: a) generation of micro-watershed layer, b) generation of R, K, LS, C layers c) generation of potential gully location, d) integration of layers e) generation of micro-watershed wise (MW wise) output of soil loss and f) reclassification of derived datasets, pair-wise comparison, and weighted overlay analysis. The GIS analyses were performed using ArcGIS9.3 and IDRISI Andes 15 Software. Digital image processing included a) preprocessing of satellite image data b) masking the image with the watershed boundary c) enhancement and visual interpretation d) Endmember selection using minimum noise fraction (MNF) and pixel purity index (PPI), e) fraction image production. For digital image processing ERDAS Imagine 9.1 and ENVI 4.5 software were used. All derived maps were projected into WGS1984 Zone 37N and held in grids of 30-m cell size. The overall methodology is illustrated in figure 3-7

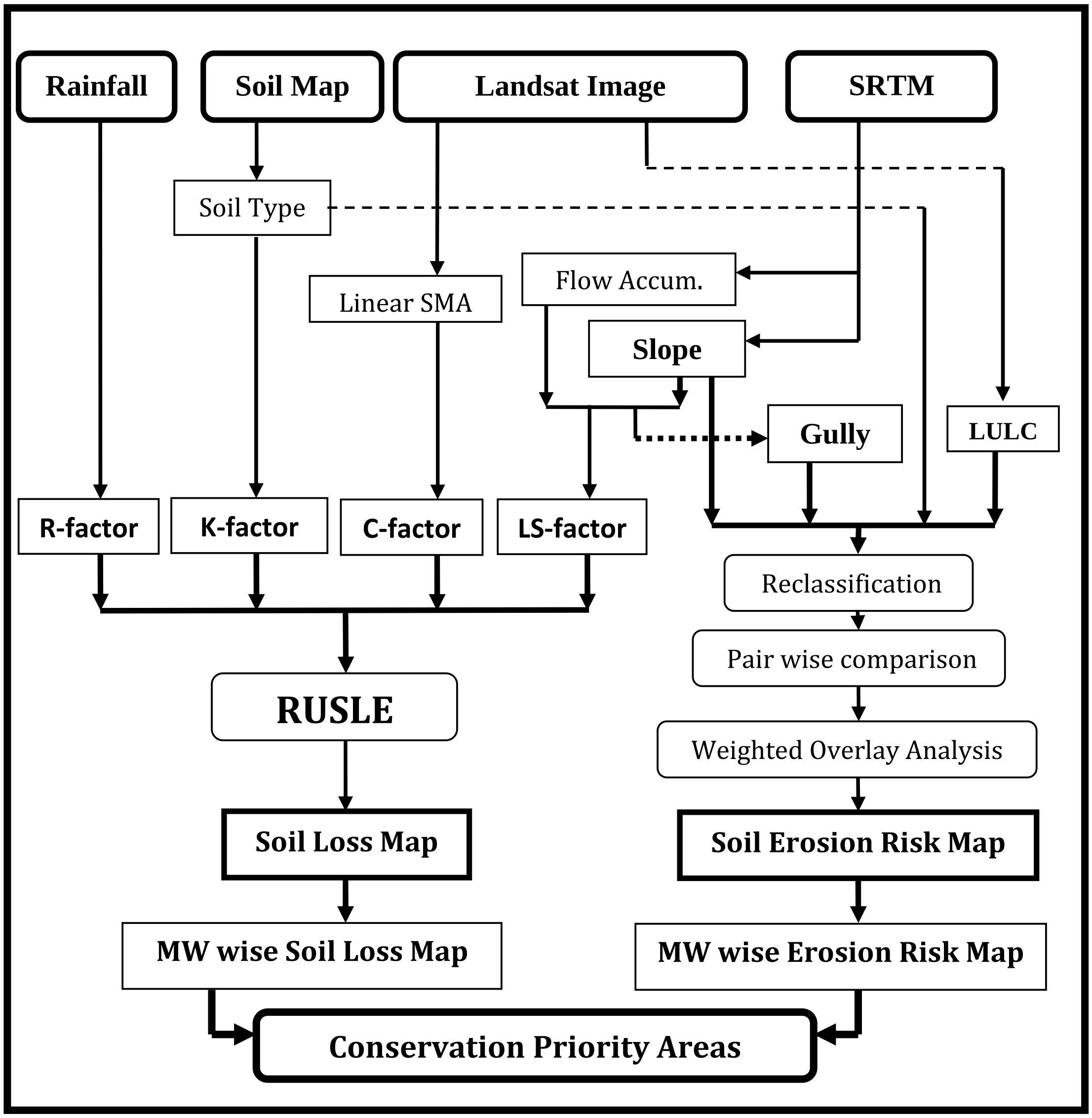


**Figure 3-7 Flow chart of the overall methodology**

## *3.3 Data Analysis*

### 3.3.1 Linear Spectral Mixture Analysis

Linear spectral unmixing has often been implemented to deal with the problem of mixed pixels. This method involves images pre-processing, image endmembers selection, image fraction production, classification of SMA fractions and finally interpretation of the fraction images.

#### *3.3.1.1 Endmember selection*

For many applications of LSMA, image endmembers are used because they can be obtained easily, representing spectra measured at the same scale as the image data. Endmembers were selected in this study by performing two consecutive steps: (1) Spectral reduction by the minimum noise fraction (MNF) transformation, and (2) Spatial reduction by the Pixel Purity Index (PPI). Using ENVE 4.5, the minimum noise fraction (MNF) algorithm was applied to the Landsat ETM+ 2005 image in which the MNF transformed data were then used as input to determine the most spectrally pure pixels (i.e. candidate end-members) in the image. In the MNF transform, the noise is separated from the data by using only the coherent portions, thus improving the spectral processing results.

Previous studies including De Asis *et al*., (2008) have shown that the use of the MNF transform can improve the quality of fraction images through decorrelation. The pixel purity index (PPI) was used in this study to find the most spectrally pure pixels in the image. The PPI stipulates how many times the pixel is extreme in the simplex. The most spectrally pure pixels typically correspond to spectrally unique materials. Hence, the pixels with the highest PPI values were selected as candidate end-members as they are linearly independent in most dimensions.

One advantage of implementing MNF-PPI is that it separates purer pixels from more mixed ones, thus reducing the number of pixels to be analyzed, which makes separation and identification of end-members more easily. The overall procedures followed in endmember selection and thus fraction image production is shown in Figure 3-8

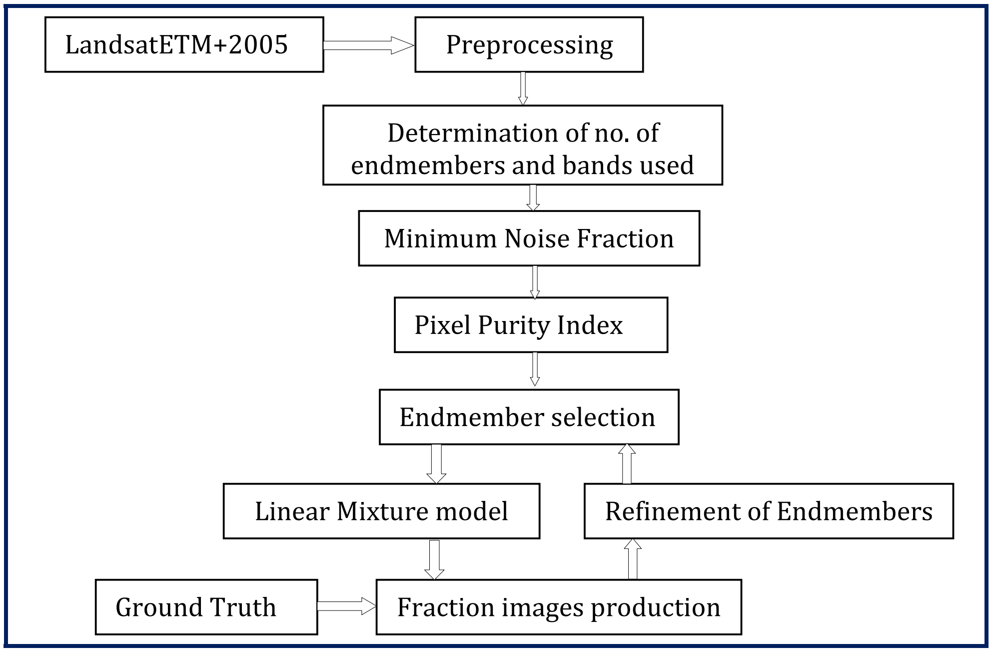


**Figure 3-8 Flowchart of Linear Spectral Mixture Analysis (Lu *et al.*, 2003a)**

Three end-members were selected: Green vegetation (GV), bare soil, and water/shadow. The average reflectance of the selected representative pixels (average of 5–12 pixels) with high PPI values that corresponded to selected end-members were used in the unmixing process in ENVI 4.5 software. The scatter plot of the selected end-members is shown in Figure 3-9.

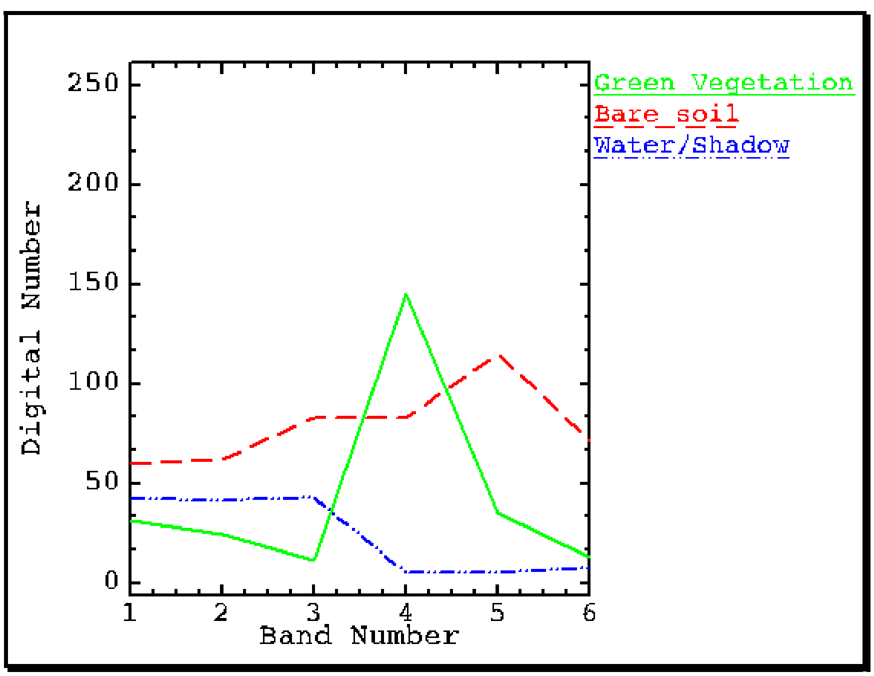


**Figure 3-9: Spectral plot of selected endmembers used in the analysis**

The green vegetation areas are characterized by a mixture of different forest tree species, and very dense shrubs, herbs. The bare soil end-member represents dirty roads and cultivated lands. The final end-member, shadow, accounts for variations in illumination caused by topography and surface textures, and tree canopy. The shade endmember was selected from the water body because it is assumed that both have similar spectral characteristics (Lillesand and Kiefer, 1999).

#### *3.3.1.2 Fraction image production*

The unmixing was done using linear spectral unmixing mapping method in ENVI 4.5. The unmixing was constrained to ensure that the fraction of any end-member lies between 0 and 1, and the sum of fractions for each pixel is equal to 1. The output of spectral unmixing consisted of the fraction image of each selected end-member (mixed vegetation, bare soil and shadow/water) and a root mean square error (RMSE). Figure 3-10 shows the fraction and RMSE images of the selected endmembers.

The fraction images (except for shadow/water) were used in determining the C factor values. Since shadow is not a physical component, it was removed with the normalization factor, $\mathbf{f = 1/ (1 - F_{shadow})}$ so that they again sum to one. This process removes only the water/shadow fraction from the image.

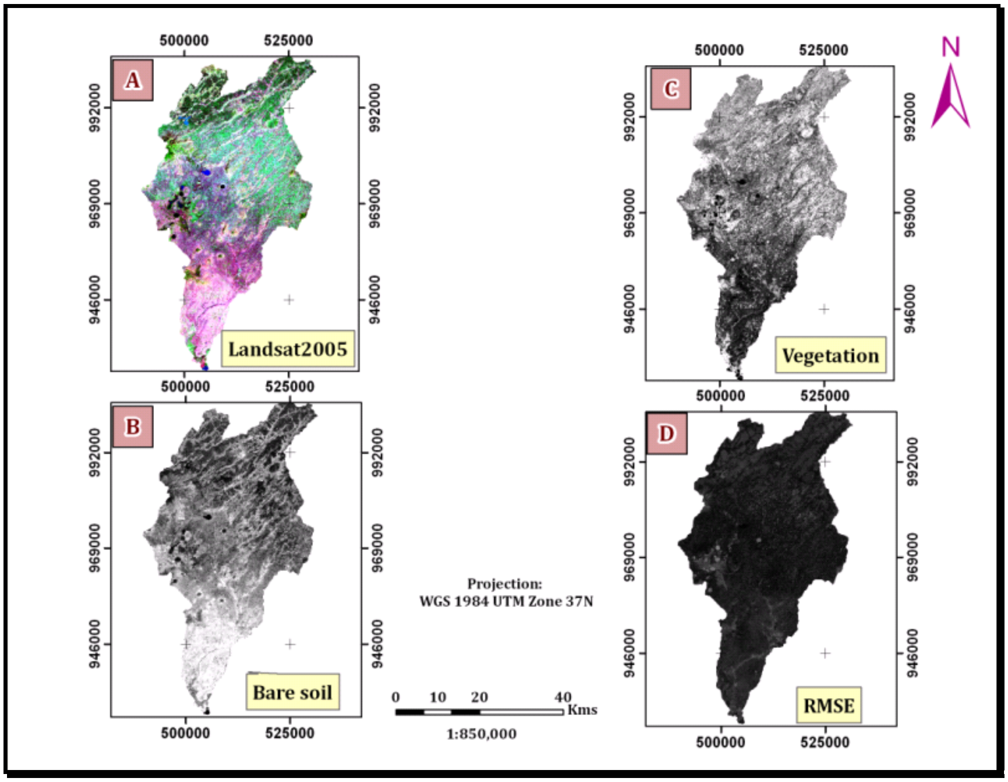


**Figure 3-10: a) Lnadsat ETM+2005 (Band 642) and b-d) Normalized fraction and RMSE images of selected endmembers for the study area.**

As discussed in Lu *et al.*, (2004b), visual analysis of fraction images is useful for understanding the characteristics of different land-cover types. The lighter the color in the fraction image of a given endmember, the higher the proportion of that end-member (and error) within the pixel. On the GV (vegetation) fraction image, for example, dense vegetation appears white owing to its high GV fraction values. Open vegetation appear bright grey. The very low GV fraction values of water and bare soils make them appear black on the GV fraction image. In contrast, on the bare soil fraction image; roads and bare soils appear white because of their high soil fraction values. Agricultural lands appear grey, dense vegetation and water areas appear black owing to their very low soil fraction values.

### 3.3.2 RUSLE Factor Generation

#### *3.3.2.1 Rainfall Erosivity (R) factor*

Soil erosion occurs when raindrops act upon the soil particles. Potential ability of rain to cause erosion is known as erosivity (R – factor) which is a function of the physical characteristics of rainfall. It is defined as the product of kinetic energy and the maximum 30 minute intensity and shows the erosivity of rainfall events (Wischmeier and Smith, 1978).

Due to rainfall characteristics and absence of automatic hourly rain intensity records in many rainfall stations in Ethiopia, it is difficult to apply erosivity equation proposed by Renard *et al.*, (1997) for Ethiopia condition(Nyssen,2001). Therefore, the erosivity factor R was calculated according to the equation given by Hurni (1985), derived from a spatial regression analysis (Hellden, 1987) for Ethiopian conditions based on the easily available mean annual rainfall (P). The R-factor is given by a regression equation as:

$$\mathbf{R = -8.12 + 0.562P}$$

Where P is the mean annual rainfall in mm

To determine the value of the R-factor in this study, the average of annual historic rainfall event (20-years) was collected from six meteorological stations located within and near the study area. Using spatial analyst extension in ArcGIS 9.3, Spline interpolation was done to generate an estimated surface from these scattered set of point data (Figure 3-11).

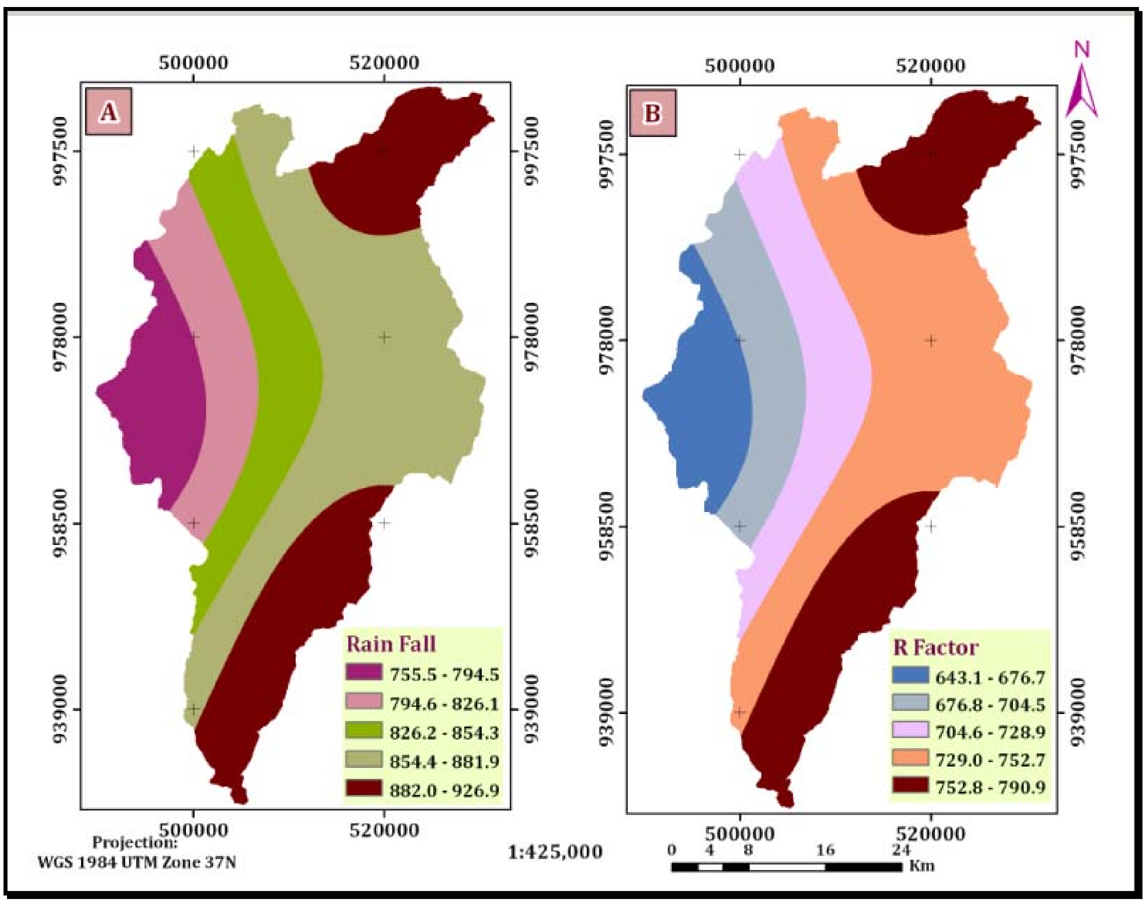


**Figure 3-11 Rainfall erosivity map**

#### *3.3.2.2 Soil Erodibility (K) factor*

Vulnerability of the soils to get eroded is referred to as erodibility of soils. The K-factor is defined as the rate of soil loss per unit of R-factor on a unit plot (Renard *et al.*, 1997). For Ethiopian condition, Hellden (1987) proposed the K values of the soil based on their color by adapting different sources (Table 3-6). Factor data for Ethiopia have been prepared by the Soil Conservation Research Project (SCRP) and are reproduced (SCRP, 1996)

**Table 3-6: Soil erodibility factor (Hellden, 1987)**

| Soil color | Black | Brown | Red | Yellow |
|---|---|---|---|---|
| K factor | 0.15 | 0.2 | 0.25 | 0.3 |

In this study, a digital soil classification map was obtained from MoWR. Five major soil categories (Table 3-7) were identified in the study area. After assigning values for each soil types the soil map was reclassified with a grid map of 30m-cell size using adopted K values (Kaltenrieder, 2007).

**Table 3-7: Soil types and their erodibility factor**

| Soil Type | Area ($km^2$) | Percentage | K factor value |
|---|---|---|---|
| **Pellic vertisols** | 687.94 | 41.8 | **0.22** |
| **Vertic cambisols** | 695.67 | 42.3 | **0.2** |
| **Chromic luvisols** | 92.4 | 5.6 | **0.2** |
| **Luvic phaezemes** | 157.1 | 9.5 | **0.16** |
| **Eutric fluvisols** | 10.8 | 0.7 | **0.28** |

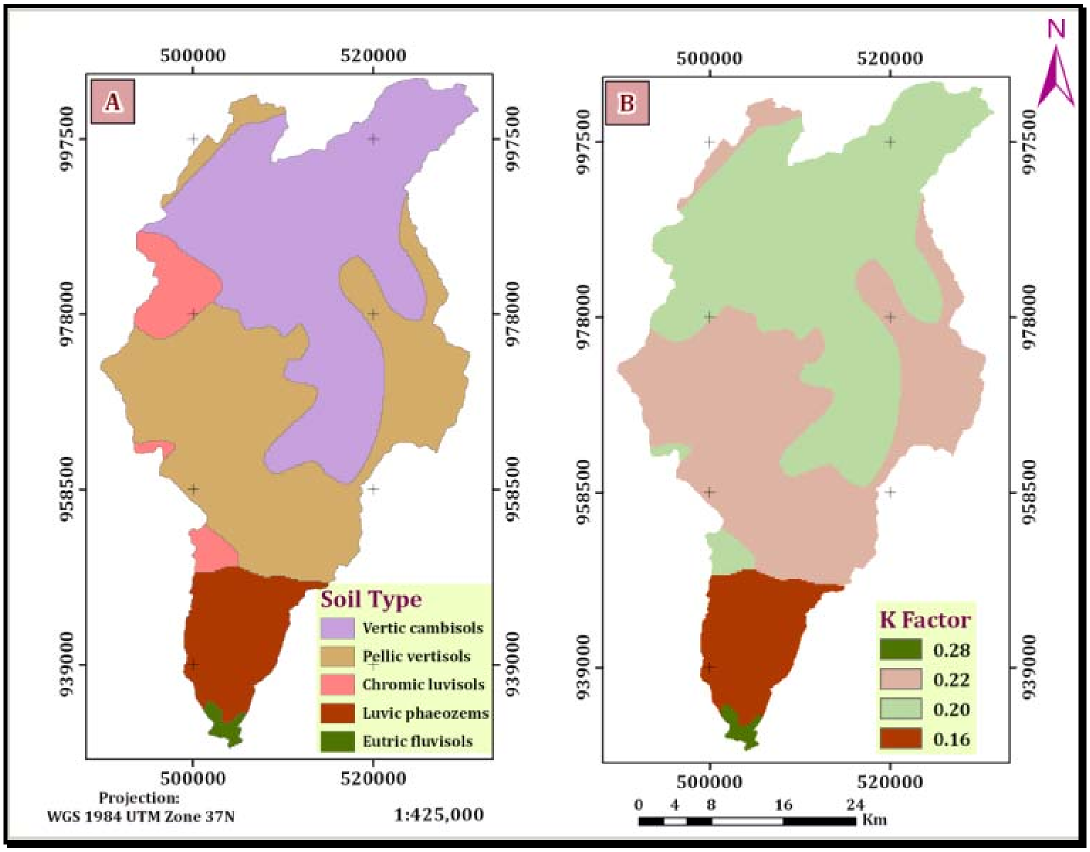


**Figure 3-12 Soil erodibility map**

#### *3.3.2.3 Topographic (LS) factors*

When using USLE or RUSLE, the effects of topography on soil erosion are estimated by the slope length (L) and slope steepness (S). In RUSLE, Slope length is defined as the horizontal distance from the origin of overland flow to the point where deposition begins or where runoff flows into a defined channel (Renard *et al.,* 1997). However, in a real two-dimensional landscape, overland flow and the resulting soil loss do not really depend upon the distance to the divide or upslope border of the field, rather on the area per unit of contour length contributing runoff to that point. For this reason, the slope length unit should be replaced by the unit-contributing area (Shi *et al.*, 2004). Upslope contributing area is the area from which the water flows into a given grid cell (Mitasova *et al.,* 1996).

DEM dataset of 30m resolution was clipped to encompass the zone of interest, and used for generating LS factor. Recent advancements in GIS technology have enabled more accurate estimation of slope length and steepness. In order to derive LS-factor values, a series of DEM-derived grids are produced using ArcGIS 9.3. As the first, any spurious single-cell sinks within the source DEM are filled to produce a depression less DEM. In this process, individual sink elevations were flattened to correspond with surrounding cells. The flow directions of each DEM cell are then calculated using the Flow direction toolset. From flow directions Flow accumulation was determined (Figure 3-13).

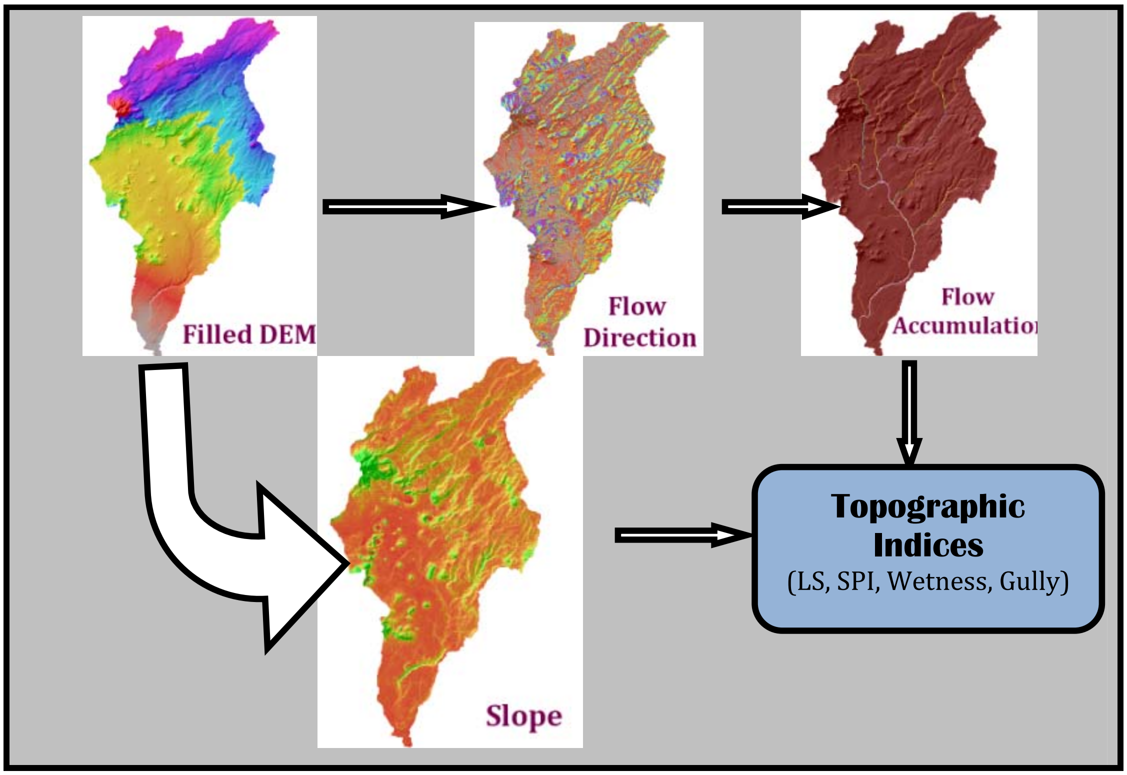


**Figure 3-13: Procedures of LS factor generation**

The slope length (L) and slope steepness (S) were calculated applying the following successive equations.

**Slope Length (L)** is given by the following expression

$$L = (\lambda/22.13)^{m} \qquad m = F/1+F \qquad F = \frac{\sin\beta/0.0896}{3(\sin\beta)^{0.8} + 0.56}$$

Using raster calculator in ArcGIS 9.3, value of F was determined using the following expression:

```
F = ((sin([slop] * 0.01745)) / 0.0896) / (3 * pow( sin([slop] * 0.01745),0.8) + 0.56))
```

Where λ is the slop length (m), m is the slope length exponent and β is slope angle.

Replacing slope length with unit contributing areas, the slope length factor L (Desmet & Govers, 1996) written as:

$$L(i, j) = \frac{(A(i, j) + D^{2})^{m+1} - A(i,j)^{m+1}}{X^{m}.\ D^{m+2}.\ (22.13)^{m}}$$

Using raster calculator in ArcGIS 9.3, value of L was determined using the following expression:

***L = (pow([Flowacc] + 900,([m] + 1)) - pow([Flowacc],[m] + 1)) / (pow(30,[m] + 2) * pow(22.13,[m]))***

Where A(i , j)[m] is unit contributing area at the inlet of grid cell, D is grid spacing which is 30m in this case and x is shape correction factor.

**Slope Steepness (S)**

$$S(i,j) = \begin{cases} 10.8\sin\beta(i,j) + 0.03, & \tan\beta(i,j) < 0.09 \\ 16.8\sin\beta(i,j) - 0.50, & \tan\beta(i,j) \geq 0.09 \end{cases}$$

Using Con toolset in ArcGIS 9.3, value of S was determined using the following expression:

***S = Con(tan([slop] * 0.01745) < 0.09,(10.8 * sin([slop] * 0.01745) + 0.03),(16.8 * sin([slop] * 0.01745) - 0.5))***

After determining the L and S for each grid cell, the LS factor was then determined by multiplying the L and S values in ArcGIS 9.3 and a map of the LS factor was produced(Figure 3-14).

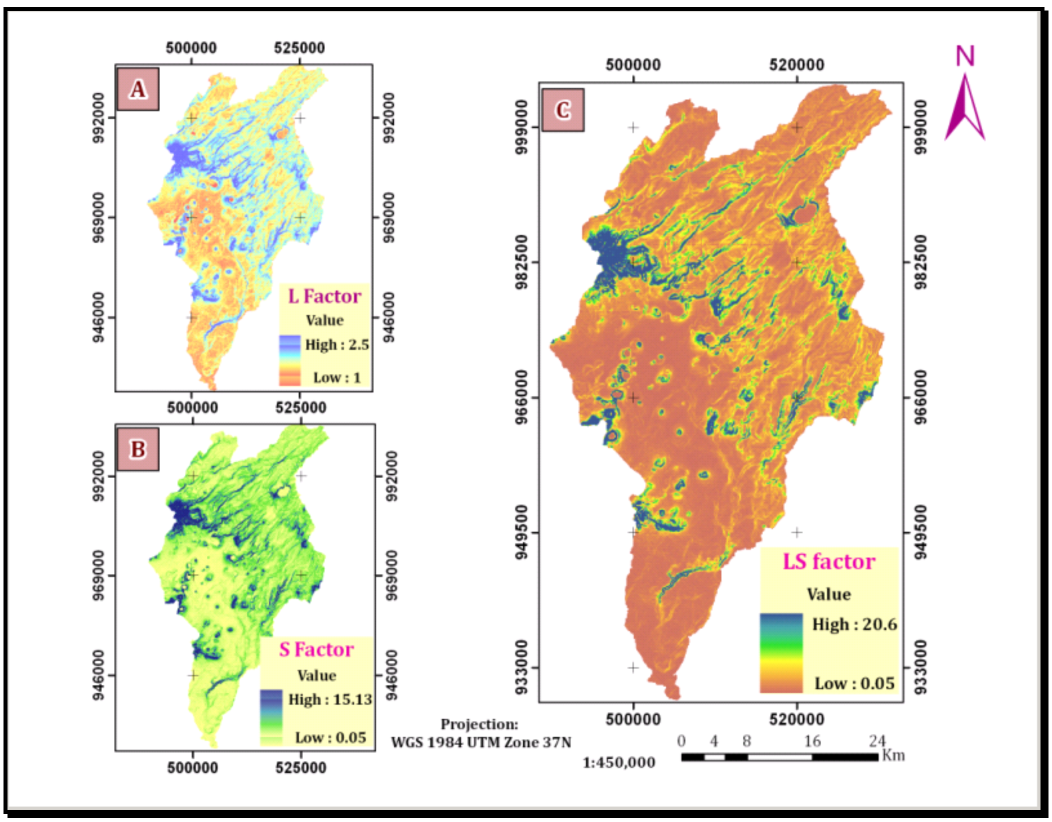


**Figure 3-14: Map of a) Slope Length (L), b) Steepness (S) and c) LS factor**

#### *3.3.2.4 Cover (C) factor*

The cover and management factor (C) reflects the effect of cropping and management practices on soil erosion rates (Renard *et al.,* 1997). The C-factor is defined as the ratio of soil loss from land with specific vegetation to the corresponding soil loss from continuous fallow (Wischmeier and Smith, 1978). Based on this concept, we used the fractional abundance of bare soil and vegetation abundance (as determined from the LSMA in section 3.3.2.2) to define a bare soil to vegetation cover ratio as an indicator of susceptibility to soil erosion on a pixel-by-pixel basis as follows:

$$\mathbf{C = F_{bs}/(1+ F_{veg})}$$

Where, $F_{bs}$ and $F_{veg}$ are the fractions of bare soil, vegetation respectively. The equation assumes that soil erosion occurs only when there are exposed soils that are subject to soil detachment by raindrop impact and surface run-off. The addition of 1.0 in the denominator limits the C value between 0 and 1. As can be seem in figure 3-15 higher values indicating more bare soil (high susceptibility to erosion) and low values corresponding to high vegetation (no soil erosion).

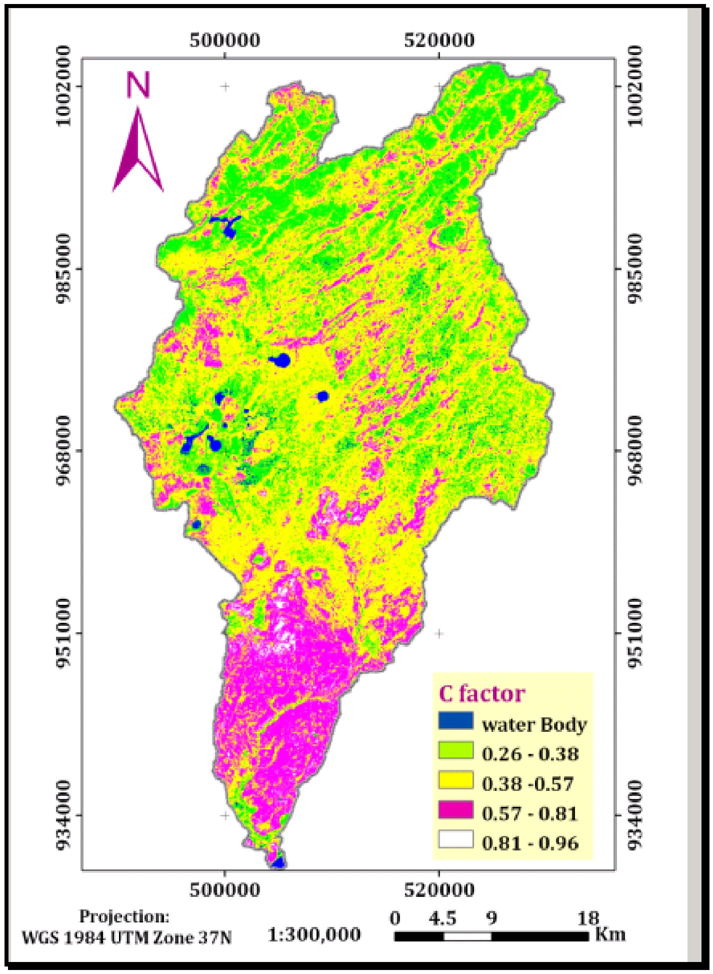


**Figure 3-15: LSMA derived C factor**

#### *3.3.2.5 Supporting conservation practice (P) factor*

Specific cultivation practices affect erosion by modifying the flow pattern and direction of runoff and by reducing the amount of runoff (Renard *et al.*, 1997). Values for this factor were assigned considering local management practices and based on values suggested in Hurni (1985). Since most soil conservation support practices being utilized in the study area are not functional due to lack of regular maintenance, the P factor was assigned to be equal to 1 for the present study.

### 3.3.3 MCA factor generation and reclassification

Multi-criteria analysis often compares various alternatives with the help of certain criteria. These criteria are often a translation of the project objectives. The outcomes are not in the form of a valuation but more often in the form of selection, classification or ranking of alternatives.

MCA can help to assess a watershed's propensity to erosion using easily available data. To perform MCA for soil risk area identification in the Mojo River Watershed, four criteria viz. slope, soil, gully location and LULC have been derived from various sources. GIS aided analysis has been done to obtain a map for each criterion. On the basis of the range (Minimum and maximum value) in 33 micro-watersheds, 5 sub-classes were formed and weights from 1 to 5 were assigned to each sub-class as per their contributions to soil losses.

#### *3.3.3.1 Slope*

As runoff velocity depends on topography in addition to the rainfall regime, slope steepness is, therefore, chosen as one of the criteria for erosivity potential estimation. As the slopes steepens, runoff and thus erosion potential increases. The slope map of the watersheds (Figure 3-16) were thus classified into five classes based on thresholds given in Lulseged and Vlek (2005) and the slope classes were ranked from 1 to 5, with 1 representing slopes with the lowest runoff potential and 5 with the highest.

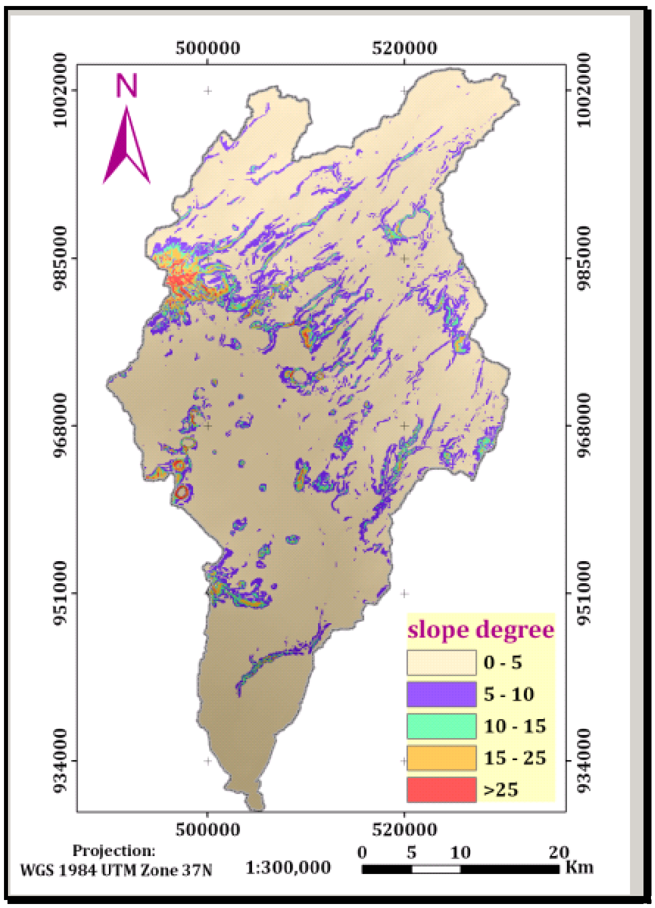


**Figure 3-16: Slope map**

#### *3.3.3.2 Potential Locations of Ephemeral Gullies*

To predict the susceptibility of a particular field to ephemeral gully formation, a threshold concept has been adopted. Generally, the gully incision is expected to appear when contributing area together with local slope exceed a given threshold (Jetten *et al*., 2006). For different environmental conditions and different gully initiating processes, different thresholds can be applied (Poesen *et al.,* 2003).

To predict the potential location and spatial patterns of gullies in the study area, the method proposed by Thorne *et al.,* (1986) and Moore *et al*., (1988) were used. As described in section 3.3.4.3, upslope contributing area or flow accumulation (As) and local slope (β) were generated from DEM of the study area. Using As and β as in input, stream power index and wetness index were then determined (Figure 3-17) in ArcGIS9.3 Spatial Analyst raster calculator using the following Equations.

***Stream Power Index (SPI):*** It is the product of watershed area and slope that indicates possible source of erosion by concentrated flow detachment risk and used to identity suitable locations for soil conservation measures to reduce concentrated surface runoff.

$$SPI = A_s \tan\beta$$

***Wetness Index (WI):*** It describes unit contributing watershed area in relation to the slope gradient. It gives an idea of the spatial distribution and zones of saturation or variable sources for runoff generation in the watershed.

$$WI = \ln(A_s / \tan\beta)$$

Where $A_s$ = the unit contributing area ($m^2/m$),

β = the local slope (m/m),

$A_s\tan\beta$ = the stream power index (SPI) and

ln(As/ tanβ) = the wetness index

As shown in Figure 3-17a, higher elevation areas have low WI values whereas lowest elevation areas high WI. Hill slopes in the watershed were characterized as low WI values indicating dry areas whereas WI values increases at lower reaches of the watershed i.e., in piedmont and flood plains indicating as possible source areas for saturated overland flow.

Hilly and upper parts of piedmont area are characterized by high SPI values showing area of high erosion. Higher SPI values has been also observed along both sides of streams in the watershed indicating possible source of soil erosion due to concentrated flow of runoff (Figure 3-17b).

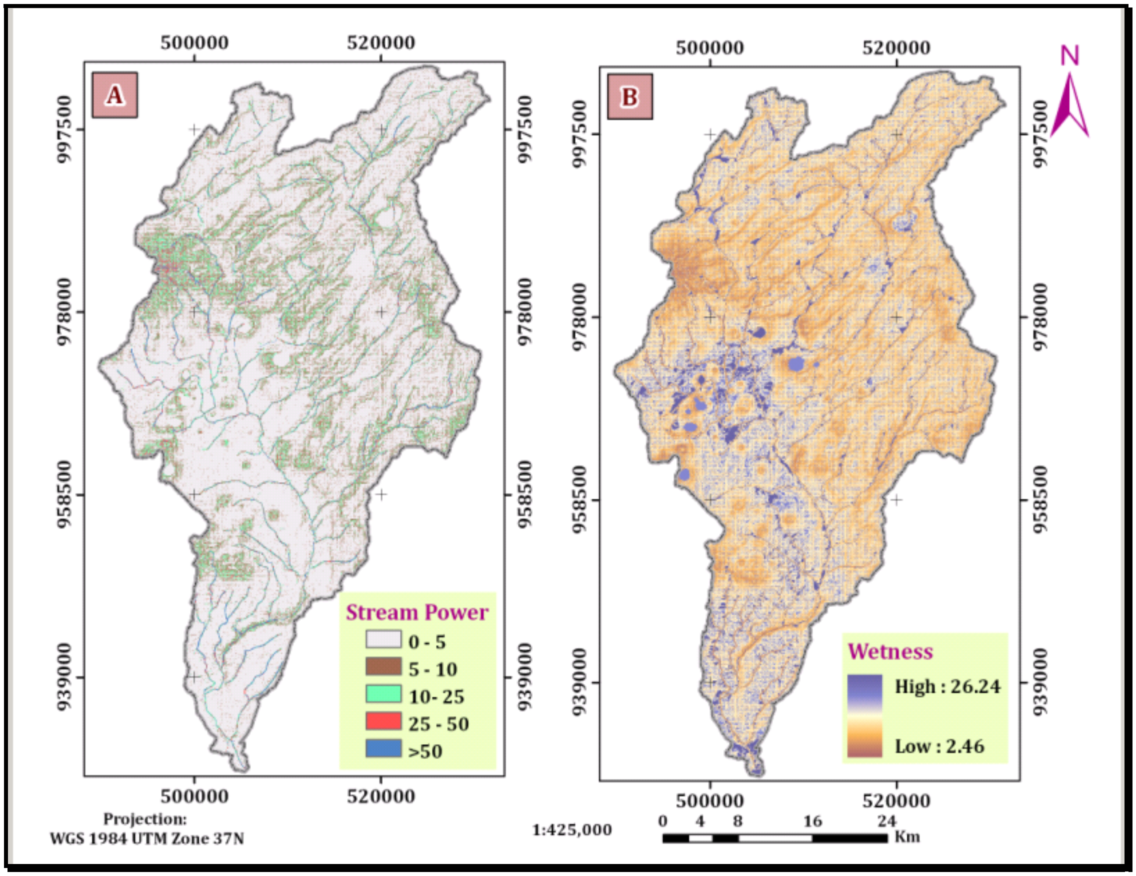


**Figure 3-17: Stream Power Index and Wetness Index**

The potential locations of ephemeral gully location may be predicted when both of the following two conditions are satisfied (Lulseged and Vlek, 2005).

$$A_s \tan\beta > 18$$

$$\ln(A_s / \tan\beta) > 6.8$$

Figure 3-18 shows critical areas for ephemeral gully formation with values 0 and 1 representing no gully and gully erosion respectively. During reclassification, potential locations for initiation of ephemeral gullies were coded as 5 whereas those with no gullies were coded as 1 with 5 indicates very high potential while 1 refers to low potential erosion.

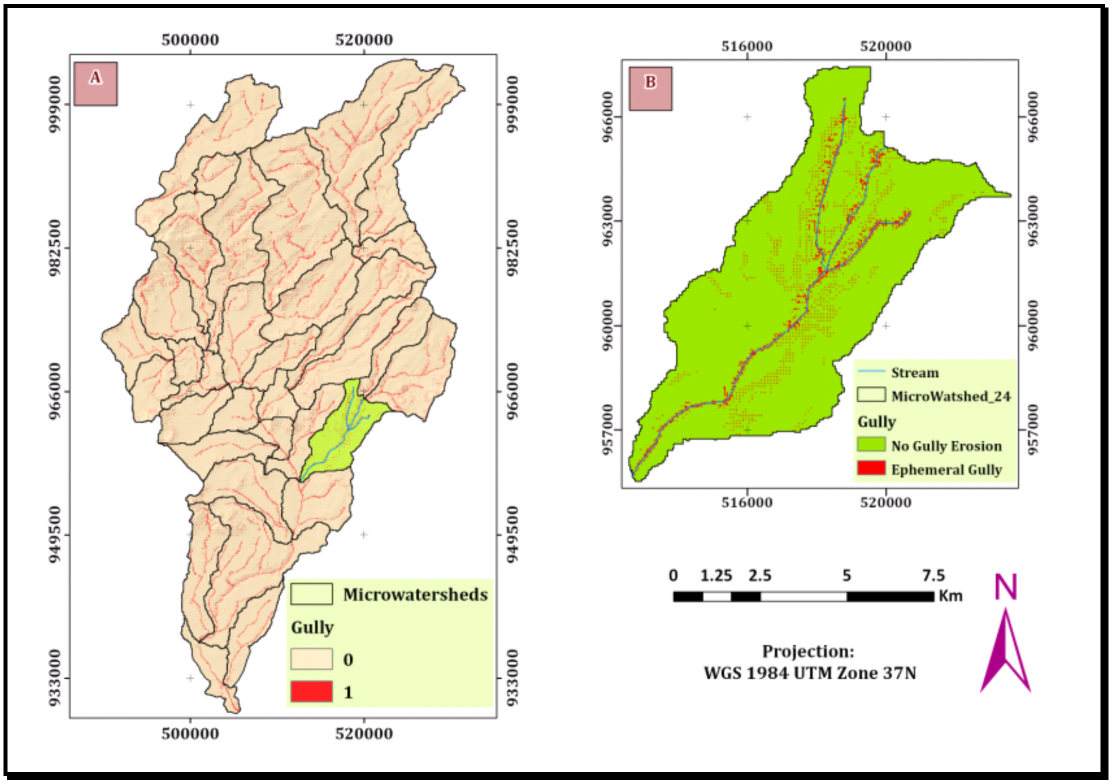


**Figure 3-18: Potential Location for Ephemeral Gully formation in: a) the whole watershed and b) Selected Micro-watershed (MW24)**

#### *3.3.3.3 Landuse/Lnadcover*

Spatial data on surface cover types enables in assessing the resistance of terrain units to erosion as a result of surface protection. Land with poor surface cover characterized by high runoff and quick response to rainfall due to low surface roughness. From visual and digital interpretations of the satellite imagery, seven major LULC categories were distinguished. Supervised land use classification method was used for land use/land cover classification (Figure 3-19). To perform MCA, areas with good surface cover were considered as sites having high erosion potential while those with poor cover assigned with high erosion potential. Table 3-9 shows general description of the landcover types in the study area.

**Table 3-9: Description and area of land cover categories**

| No | Landcover category | General description |
|---|---|---|
| 1 | Mixed forest | Areas covered with relatively tall and dense trees forming closed canopies including *Acacia albida*, *Acacia abyssinica*, *Acacia seyal*, and other remnant trees. |
| 2 | Shrub land | Areas covered with small trees, bushes and shrubs, mainly *Dodonia viscose, Carissa edulis, Otostegia integrifolia, Rhus retinorrhoea, Osyris compressa, Myrsine africana, Euclea shimperi* and *Erica arborea* with less crown cover. |
| 3 | Crop land | Areas currently under crops (rain-fed or irrigated crops). This class may include small inter-field cover types (e.g. hedges, grass strips, small windbreaks, etc.) |
| 4 | Fallow land | Areas of land un-ploughed/ploughed for growing rain-fed or irrigated crops. This category includes land that has not been planted or sown with crops currently. |
| 5 | Bare land | Areas with degraded lands (gullies), bare ground or inundation areas |
| 6 | Built-up areas | Areas under residential or industrial places |
| 7 | Water body | Areas under natural lakes, wetlands, rivers and manmade small dams |

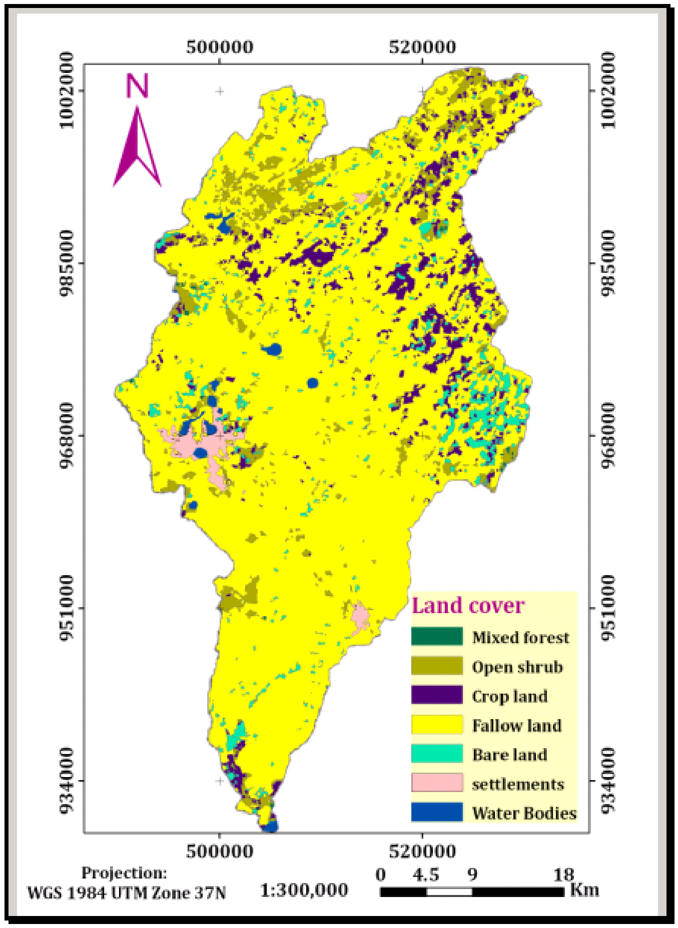


**Figure 3-19: Land use/Land cover map**

### *3.3.3.1 Soil*

To consider the pedological effect on soil erosion in the study area, soil erodibility also taken as one factor for MCA. Erodibility refers vulnerability of the soils to get eroded. Soils of the study area were ranked based on their K factor. Those soils types having low K factor value are less susceptible to soil erosion and thus were assigned 1 and those soils having high K value were assigned 5.

### *3.3.3.2 Reclassification of the datasets*

The maps of slope, soil, gully location and landuse/landcover of the study area were thus classified into five cardinal classes based on thresholds given in different literatures (Lulseged and Vlek, 2005; Trimphati,*et al.*, 2003; Deore, 2005). Classes were ranked from 1 to 5, with 1 representing lowest erosion potential and 5 with the highest (Table 3-10).

**Table 3-10: Classification of parameters used in MCA to generate Composite Erosion Index**

| Rank | Erosion Class | Parameters | | | |
|---|---|---|---|---|---|
| | | Slope | Soil Type | Land cover | Gully |
| 1 | Very low | $0\text{-}5^0$ | Luvic phaezemes (K=0.16) | Mixed forest | No gully |
| 2 | Low | $5\text{-}10^0$ | Vertic cambisols/ Chromic luvisols(K=0.20) | Open shrub | |
| 3 | Medium | $10\text{-}15^0$ | Pellic vertisols (K=0.22) | Crop land | |
| 4 | High | $15\text{-}25^0$ | Eutric fluvisols (K=0.28) | Fallow | |
| 5 | Very high | $>25^0$ | | Bare land | Gullies |

#### *3.3.3.3 Pairwise comparison for weighting*

A weight is a value assigned to an evaluation criterion which indicates its importance relative to other criteria under consideration (Jankowski, 1995). For assigning weights in this study, pairwise comparison method was used so as to reduce the complexity of decision making since two components are considered at a time. Pairwise comparison method involves 3 steps: (1) development of a comparison matrix (2) computation of weights for each element of the hierarchy and (3) estimation of consistency ratio. IDRISI Andes 15 software was used to generate the weight for pairwise comparison (Table 3-11).

**Table 3-11: Pairwise weights**

| Criteria | Weight |
|---|---|
| **Slope** | 0.3516 |
| **Gully** | 0.2915 |
| **Landcover** | 0.2336 |
| **Soil** | 0.1233 |

Consistency ratio = 0.07

The Consistency Ratio of <0.1, is considered satisfactory and, therefore, the pairwise weights were accepted for further MCA to calculate erosion intensity in the study area.

# 4 RESULTS AND DISCUSSION

## 4.1 Potential soil loss in the watershed

The RUSLE model was run within the ArcGIS by multiplying the six factors (RKLSCP) in the raster calculator. The quantitative output of predicted soil loss rates for the Mojo River Watershed resulting from current farming practices were computed and grouped into five ordinal classes and displayed on the map. Based on the analysis, the total amount of soil loss in the Mojo River Watershed is about 9,883,473.4 tons per year from 1645.77 km$^2$. As shown in Figure 4-1 and Table 4-1, the amount of soil loss of each parcel of land in the watersheds ranges from 8.57 to 134.46t/ha/year. The mean annual soil loss of the area is 21.2t/ha/year. According to the estimate of FAO (1984), the annual soil loss of the highlands of Ethiopia ranges from 1248 – 23400 million ton per year from 78 million of hectare of pasture, ranges and cultivated fields throughout Ethiopia.

**Table 4-1: Area and proportion of each soil erosion class**

| Soil erosion class | Numerical range (t/ ha/yr) | Area | |
|---|---|---|---|
| | | (Km²) | (%) |
| Very low | 8.6- 14.7 | 57.36 | 3.49 |
| Low | 14.7 - 37.3 | 487.50 | 29.62 |
| Moderate | 37.3 - 59.9 | 716.51 | 43.54 |
| High | 59.9 - 82.6 | 323.64 | 19.67 |
| Very high | 82.6- 134.5 | 60.75 | 3.69 |
| | **Total** | **1645.77** | **100** |

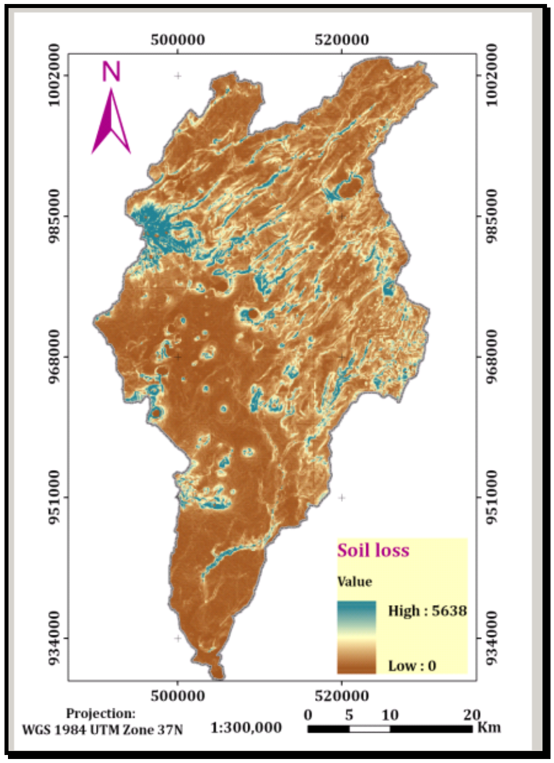


**Figure 4-1: Soil loss map of the study area**

Previous studies conducted on soil erosion assessment in Ethiopia shows different rate of soil erosion. For example, studies conducted by FAO, (1986), in the Ethiopian high lands shows 100t/ha/yr soil loss from cropped lands taking in to consideration the redeposit. Another study conducted by Soil Conservation Research Program (SCRP) at Anjeni research station revealed that the annual soil loss rate to be 131 - 170 t/ha (SCRP, 1996).

The average annual soil loss in Awash River basin is in the order of 200-300 t/ha (PDRE, 1989). According to MoWR, (2008), estimates for soil erosion based on the sediment curve at Mojo gauging station and on an average sedimentation rating in Koka reservoir are an order of magnitude higher at 15-25 ton/ha/year. Removal of vegetation cover through deforestation and overgrazing, repeated tilling of the soil to prepare fine seedbed and lack of adequate soil and water conservation resulting in such loss and causing Koka dam to silt up. This has lowered the water volume of the dam from its designed live storage capacity of 1,667 $Mm^3$ to 1,186 $Mm^3$ at present (i.e., loss of 481 $Mm^3$), which is a loss of 30% of the total storage volume of the reservoir (EEPC, 2002; Eyasu, 2003). In addition, erosion causes a decline in crop yields primarily by reducing rooting depth, water holding capacity and loss of nutrients and organic matter through selective removal of the most fertile soil particles. National level estimates reveal 2% average annual reduction of the agricultural GDP due to erosion (FAO, 1986).

### 4.1.1 Prioritization of Micro-watersheds Based on Potential Soil Loss

A particular sub-watershed may get top priority due to various reasons but often, the intensity of land degradation is taken as the basis (Trimphati, *et al.*, 2003). In this study, prioritization of MWs has been done on the basis of annual soil loss. Estimated values of micro-watershed wise soil loss are classified on the basis of mean and standard deviation. The Table 4-1 & 4-2 and Figure 4-2 indicates distribution of the 33MWs according to soil loss intensity.

**Table 4-2: Ranked Microwatersheds based on potential soil loss**

| Rank | Micro-watershed | Area ($Km^2$) | Mean loss(t/ha/yr) |
|---|---|---|---|
| 1 | 6 | 60.75 | 134.46 |
| 2 | 20 | 65.92 | 70.40 |
| 3 | 9 | 66.05 | 69.22 |
| 4 | 7 | 86.96 | 64.82 |
| 5 | 12 | 57.56 | 64.18 |
| 6 | 25 | 15.46 | 62.80 |
| 7 | 14 | 31.36 | 62.52 |
| 8 | 24 | 50.54 | 59.49 |
| 9 | 4 | 131.88 | 58.35 |
| 10 | 8 | 23.98 | 54.38 |
| 11 | 10 | 59.82 | 53.26 |
| 12 | 15 | 60.98 | 49.58 |
| 13 | 18 | 28.47 | 46.60 |
| 14 | 21 | 33.71 | 46.50 |
| 15 | 26 | 33.70 | 44.88 |
| 14 | 23 | 17.30 | 43.51 |
| 17 | 2 | 91.43 | 41.72 |
| 18 | 3 | 78.55 | 41.32 |
| 19 | 30 | 104.71 | 38.46 |
| 20 | 1 | 111.88 | 36.35 |
| 21 | 11 | 51.33 | 35.68 |
| 22 | 28 | 48.28 | 35.26 |
| 23 | 31 | 48.36 | 34.68 |
| 24 | 29 | 53.10 | 34.25 |
| 25 | 17 | 17.76 | 33.87 |
| 26 | 19 | 29.78 | 33.62 |
| 27 | 13 | 16.57 | 28.34 |
| 28 | 5 | 20.08 | 25.10 |
| 29 | 27 | 35.28 | 19.15 |
| 30 | 16 | 33.14 | 18.08 |

| | | | |
|---|---|---|---|
| **31** | **22** | 21.55 | 17.72 |
| **32** | **33** | 32.85 | 12.54 |
| **33** | **32** | 24.11 | 8.57 |

**Table 4-3: Classification of micro-watersheds based on soil loss**

| Soil erosion class | Mean soil loss (t/ ha/yr) | Micro-watersheds | No. of MWs | Area | |
|---|---|---|---|---|---|
| | | | | (Km²) | (%) |
| Very low | 8.6- 14.7 | 32,33 | 2 | 57.36 | 3.49 |
| Low | 14.7 - 37.3 | 1,5,11,13,16,17,19,22,27-29,31 | 12 | 487.50 | 29.62 |
| Moderate | 37.3 - 59.9 | 2-4,8,10,15,18,21,23,24,26,30 | 12 | 716.51 | 43.54 |
| High | 59.9 - 82.6 | 7,9,12,14,20,25 | 6 | 323.64 | 19.67 |
| Very high | 82.6- 134.5 | 6 | 1 | 60.75 | 3.69 |
| | | **Total** | **33** | **1645.77** | **100** |

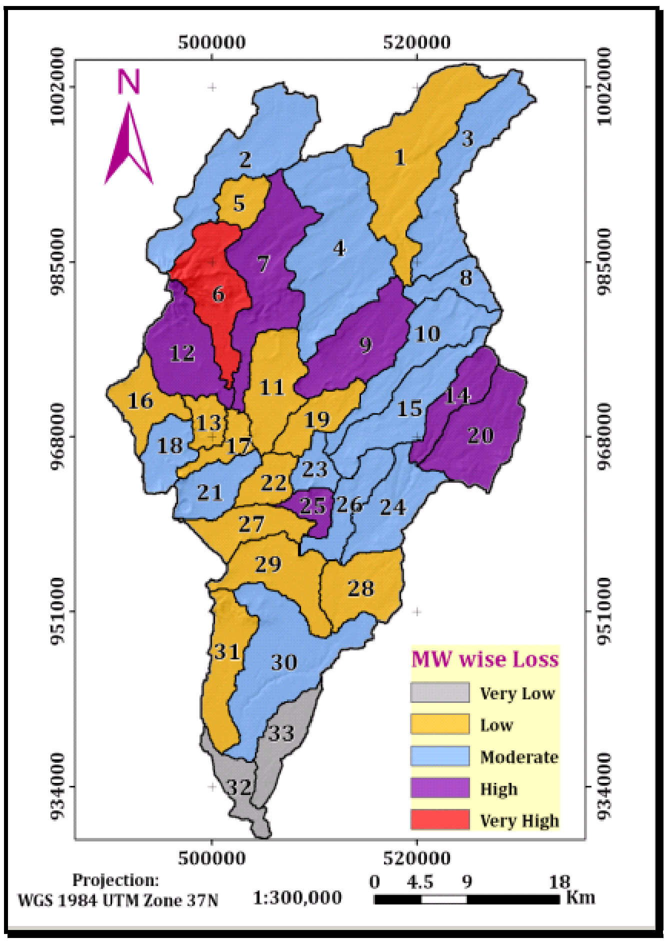


**Figure 4-2: Micro-watershed wise soil loss map**

The result showed that very high soil loss (82.6- 134.5/ha/yr) is observed in the valley as well as in the ridges of the Mojo River Watershed. Out of the 33 micro-watersheds, only one MW (MW6) experiences very high erosion rate with high contribution from C and LS factors. This

MW found in the upper part of the watersheds. Six MWs (7, 9, 12, 14, 20, and 25) fell under high soil erosion classes (59.9 - 82.6t/ha/yr). Very low soil loss category (8.6- 14.7t/ha/yr) includes 2 MWs (32 and 33) which are located in the lower reach (southern part) of the study area. This may be due to the low average surface slope of less than 5% with plain topography. About 40% of the micro-watersheds fall in below the annual average soil loss of the entire watersheds.

On the basis of annual soil losses, micro-watersheds (6, 7, 9, 12, 14, 20, and 25) were found to be critical. After arranging the critical micro-watersheds in ascending order, considering the annual soil losses from each micro-watershed, priorities were fixed. The micro -watershed that comes first is given the top priority for developing the management plan to reduce the soil and nutrient losses. As a result the critical sub-watersheds MW6, MW20, MW9 MW7, MW12, MW25 and MW14 with annual average soil loss between 59.9 and 134.5t/ha/yr were selected and recommended to adopt the management measures in that order to reduce the soil losses and to conserve the resources within the watershed.

### 4.1.2 Contribution of Erosion Factors

Soil loss in different landforms of the study watershed is influenced by erosion factors differently. For instance, landforms with well land cover indicated less soil loss. Because it dissipates the energy from rain drops and also decreases the volume and velocity of runoff effect. Soil loss estimated from landforms with very steep slope (> 30%) in the study watershed is smaller than slopes in the rage of 2-10% and 10-15%. The reason is the cover factor is better in the very steeper slopes of the watershed. This includes less human and livestock interferences and relatively better vegetation cover of bushes and shrubs due to area closure. Table 4-3 shows estimated area of the study area based on mean soil loss in relation to the prevailing slope steepness. More than 13% (223.3 km$^2$) of the study area reports high erosion rate (82.6- 134.5t/ha/yr) within 2-10% slope gradient (gently to undulating flat surface).

**Table 4-4: Tabulated area of mean soil loss within existing slope gradients**

| Slope % | Annual Soil loss t/ha/yr | | | | | Total(Km$^2$) |
|---|---|---|---|---|---|---|
| | *8.6- 14.7* | *14.7 - 37.3* | *37.3 - 59.9* | *59.9 - 82.6* | *82.6- 134.5* | |
| **0 -2** | 74.35 | 119.40 | 100.21 | 90.34 | 35.88 | 420.18 |
| **2-10** | 36.12 | 207.67 | 380.60 | 153.14 | **223.25** | 1000.78 |
| **10-15** | 0.64 | 16.22 | 33.31 | 19.71 | 40.45 | 110.32 |
| **15-30** | 0.66 | 14.78 | 17.89 | 18.49 | 33.81 | 85.64 |
| **>30** | 0.01 | 3.73 | 1.82 | 8.81 | 12.24 | 26.62 |

| | | | | | | |
|---|---|---|---|---|---|---|
| **Total ($Km^2$)** | **111.78** | **361.80** | **533.83** | **290.49** | **345.64** | **1645.77** |

The major concern in soil loss estimation is the accuracy of the estimated values for the factors used in the RUSLE. The RUSLE model requires six input data layers be multiplied, and the inherent errors in each layer when multiplied, contribute to an even greater uncertainty in the derived soil loss values. RUSLE model's role as priority area identification tool (in this study), is for relative comparisons among land areas which are more critical than assessing the absolute soil loss in a particular cell.

## *4.2 Potential locations for ephemeral gully formation*

Topographic thresholds for gully initiation and location have been explained mainly in terms of soil surface gradient (β) and critical drainage area (*As*) relations (Poesen *et al.,* 2003). Based on the method proposed by Thorne *et al*., (1986) and Moore *et al.,* (1988), SPI and WI maps were generated as described in section 3.3.3.2. To predict potential spatial patterns of ephemeral gullies in the study area, SPI and WI above a threshold values were estimated and crossed with "AND" Boolean operation in ArcGIS 9.3 raster calculator using the expression: **"SPI > 17 AND WI > 6.5".** The resulted map shows areas with values 0 and 1 indicating areas with no gully and with gully erosion respectively.

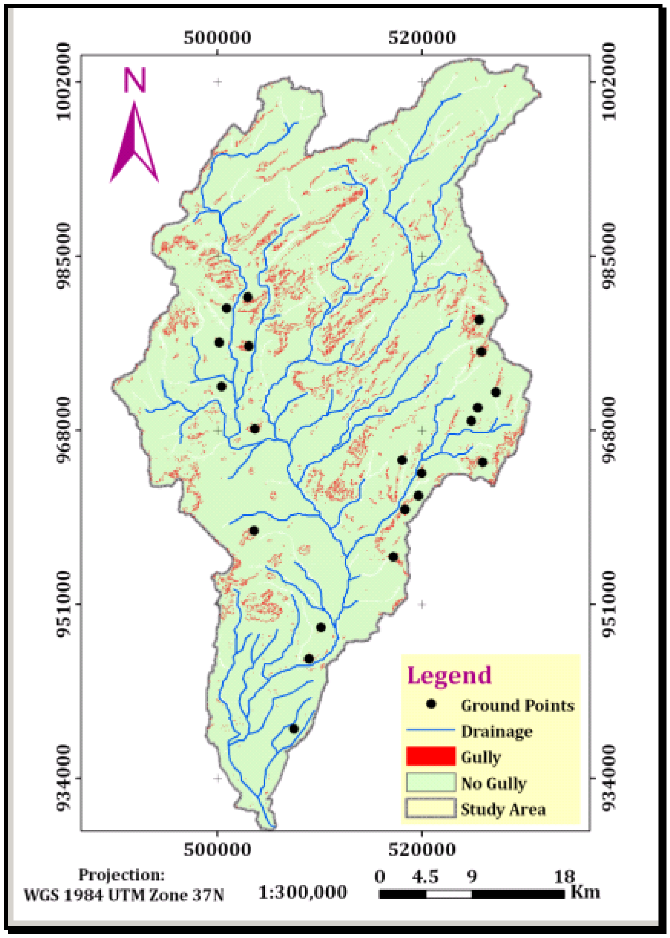


**Figure 4-3: Spatial location of ephemeral gullies in the study area**

Based on the result obtained, 94.9% (1578.81km$^2$) of the study area is with no gully and the remaining 5.1% (66.96km$^2$) is with gully erosion. According to land use/cover classified map, most of the ephemeral gullies were found in agriculture areas which are located in the upper and central parts of study area (Figure 4-3). Field studies also revealed that agriculture areas really have a lot of gully erosion. However, in vegetated areas especially sparse vegetation were also found gully erosion because of poor ground cover. For validation, gully location maps were crossed with 21 ground points as illustrated in Figure 4-3. The Contingency matrix (Table 4-4) showed the overall accuracy of 71.4% for predicting potential gully location. This result explained that SPI and WI with the threshold values 17 and 6.5 respectively seemed to be somewhat acceptable for predicting potential areas for ephemeral gully location in the study area. However, sufficient validation points will be required to eliminate those small ephemeral gullies that were observed, mainly in the upslope parts of the watershed.

**Table 4-5: Contingency matrix for gully location using ground truth data**

| Areas | Reference from field work | Total |
|---|---|---|
| | **Gully** | |
| Gully | 16 | 17 |
| No gully | 5 | 4 |
| **Total** | 21 | 21 |
| Overall Accuracy = (16/21) *100 = 71.4% | | |

Previous studies cited in Poesen *et al.,* (1996) have shown that percentage of total soil loss due to ephemeral gully erosion ranges between 10 and 46%. Assessments of gully erosion volumes in Ethiopia are rare. Using photogrammetric techniques, Shibru *et al.,* (2003) estimate that between 1966 and 1996, 700,000 tons of soils were lost by gully erosion from a 9-$km^2$ watershed in the eastern highlands (26t/ha/yr). Using monitoring and interview techniques to establish average long-term soil loss rates by gully erosion in Central Tigray, Nyssen (2001) obtained 5t/ha/yr.

## *4.3 Erosion Risk in the Watershed based on MCE*

### 4.3.1 Composite Erosion Index (CEI)

All criteria layers obtained in section 3.3.3 were multiplied by an appropriate weight derived from pairwise comparison of criteria (Table 4-2) and then added by Weighted Linear Combination (WLC) equation in raster calculator operation (ArcGIS9.3).

The algebraic operation performed on four layers is as follow:

$$CEI = (W_1*S) + (W_2*LC) + (W_3*St) + (W_4*G)$$

Where CEI is Composite Erosion Index;

$W_1$, $W_2$----$W_4$ are pairwise weights derived from AHP; and

S, LC, St and G are reclassified slope, landcover, soil type and gully.

The final output map indicates micro-watershedwise CEI that relates to the erosion intensity of the area under the relative contribution of the given criteria. Values of CEI range between 0.89 and 4.52 (Figure 4-4).

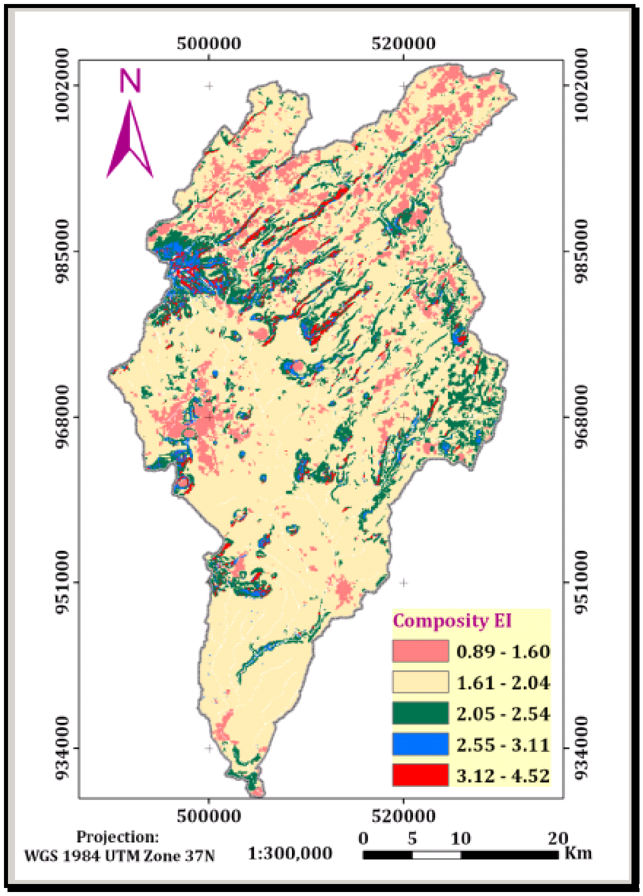


**Figure 4-4: Composite Erosion Index map**

Figure 4-4 showed the influence of topography and gully on erosion potential in the study area. Minimal and low erosion potential was present under dense vegetation when the slope gradient was also low, but increased with higher slope values. There were few cells with extreme erosion potential, and these were usually restricted along stream channels and ridges with very high slope values. Table 4-6 shows area and proportion of the study area categorized in a classified CEI map. Most of the study area (69.1%) lays on CEI class values between 1.62 and 2.04.

**Table 4-6: Areal proportion of the study area based on CEI classes**

| Erosion Intensity class | Area | |
|---|---|---|
| | Km$^2$ | Percent |
| 0.89-1.60 | 177.30 | 10.97 |
| 1.61-2.04 | 1116.50 | 69.10 |
| 2.05-2.54 | 244.26 | 15.12 |
| 2.55-3.11 | 37.66 | 2.33 |
| 3.12-4.52 | 40.03 | 2.48 |
| **Total** | **1645.77** | **100** |

### 4.3.2 Micro-watershed prioritization based on CEI

The intensity of soil erosion indicated by Composite Erosion Index in the MWs is considered for their prioritization for selection and implementation of conservation measures and plan appropriate landuse to minimize the soil losses in them. All 33 micro-watershed were grouped into five CEI classes based on mean (1.93) and standard deviation (0.11). CEI ranges between 1.68 (MW5) and 2.20(MW6) (Table 4-7 and Figure 4-4)

**Table 4-7: Micro-watershed wise erosion intensity based on CIE**

| Rank | Micro-watershed | Area ($Km^2$) | CEI |
|---|---|---|---|
| 1 | 6 | 60.75 | 2.20 |
| 2 | 20 | 66.17 | 2.06 |
| 3 | 12 | 57.57 | 2.05 |
| 4 | 9 | 66.05 | 2.05 |
| 5 | 25 | 15.46 | 2.05 |
| 6 | 14 | 31.43 | 2.03 |
| 7 | 7 | 86.96 | 2.02 |
| 8 | 29 | 53.11 | 2.01 |
| 9 | 24 | 50.69 | 1.99 |
| 10 | 11 | 51.33 | 1.99 |
| 11 | 21 | 33.71 | 1.98 |
| 12 | 16 | 33.20 | 1.97 |
| 13 | 23 | 17.30 | 1.96 |
| 14 | 26 | 33.70 | 1.96 |
| 15 | 27 | 35.46 | 1.95 |
| 14 | 4 | 131.88 | 1.95 |
| 17 | 10 | 59.91 | 1.95 |
| 18 | 22 | 21.55 | 1.95 |
| 19 | 19 | 29.78 | 1.95 |
| 20 | 28 | 48.33 | 1.95 |
| 21 | 8 | 24.06 | 1.92 |
| 22 | 2 | 91.66 | 1.90 |
| 23 | 15 | 60.98 | 1.90 |
| 24 | 17 | 17.76 | 1.89 |
| 25 | 18 | 28.53 | 1.88 |
| 26 | 31 | 48.39 | 1.84 |
| 27 | 30 | 104.98 | 1.83 |
| 28 | 3 | 79.10 | 1.80 |
| 29 | 1 | 111.93 | 1.78 |
| 30 | 32 | 24.28 | 1.75 |
| 31 | 13 | 16.57 | 1.74 |
| 32 | 33 | 33.08 | 1.71 |
| 33 | 5 | 20.08 | 1.68 |

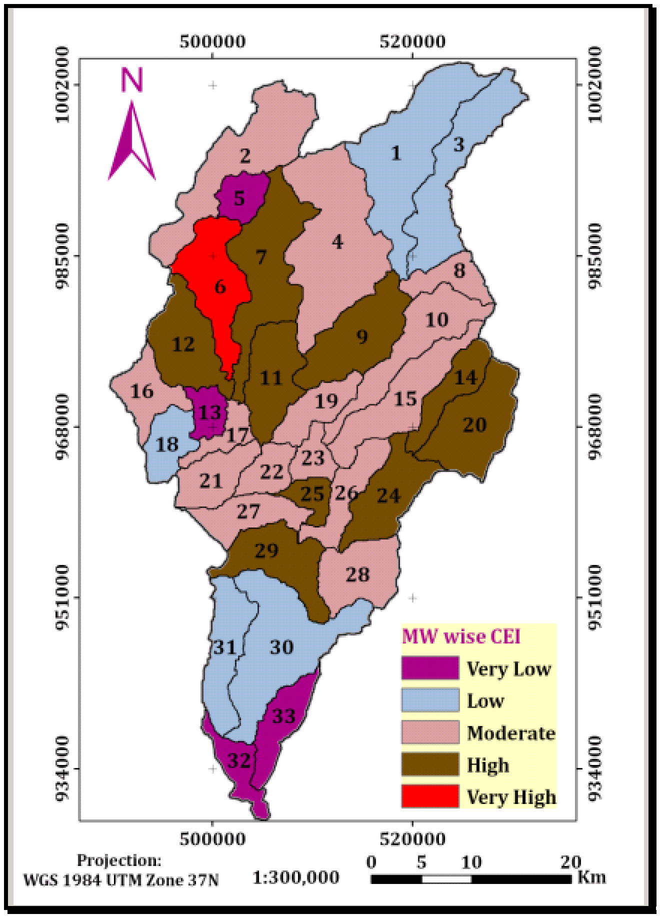


**Figure 4-5: Micro-watershed wise Composite Erosion Index map**

Micro-watershedwise CEI is presented in Table 4-8 indicates that only MWs 6 is under 'Very high' category with CEI value above 2.11. The area covered under this category is 60.75 Km$^2$ (3.69%). It is important to note that this micro-watershed is characterized by high slope gradient. 'High' category is represented by 9 MWs (29.09%) covering 478.77 Km$^2$ area. Most parts of these micro-watersheds are under cultivated and bare land and high proportion of ephemeral gullies which causing high erosion intensity. Their location is also observed on various topographic units from ridge to valley.

**Table 4-8: Categorization and prioritization of MWs based on CEI**

| CEI class | Mean CEI | Micro-watersheds | No. of MWs | Area (Km²) | Area (%) |
|---|---|---|---|---|---|
| Very low | 1.68 - 1.77 | 5,13,32,33 | 4 | 94.02 | 5.71 |
| Low | 1.78 – 1.88 | 1,3,18,30.31 | 5 | 372.92 | 22.66 |
| Moderate | 1.89 – 1.99 | 2,4,8,10,15-17,19,21-23,26-28 | 14 | 639.30 | 38.85 |
| High | 2.0 – 2.10 | 7,9,11,12,14,20,24,25,29 | 9 | 478.77 | 29.09 |
| Very high | 2.11 – 2.20 | 6 | 1 | 60.75 | 3.69 |
| | | **Total** | **33** | **1645.77** | **100** |

Among 33 MWs, about 19 MWs (39.4 %) occupying 984.36 $Km^2$ (59.8%) area of the study area experience ≤ average (≤ 1.93) erosion intensity.

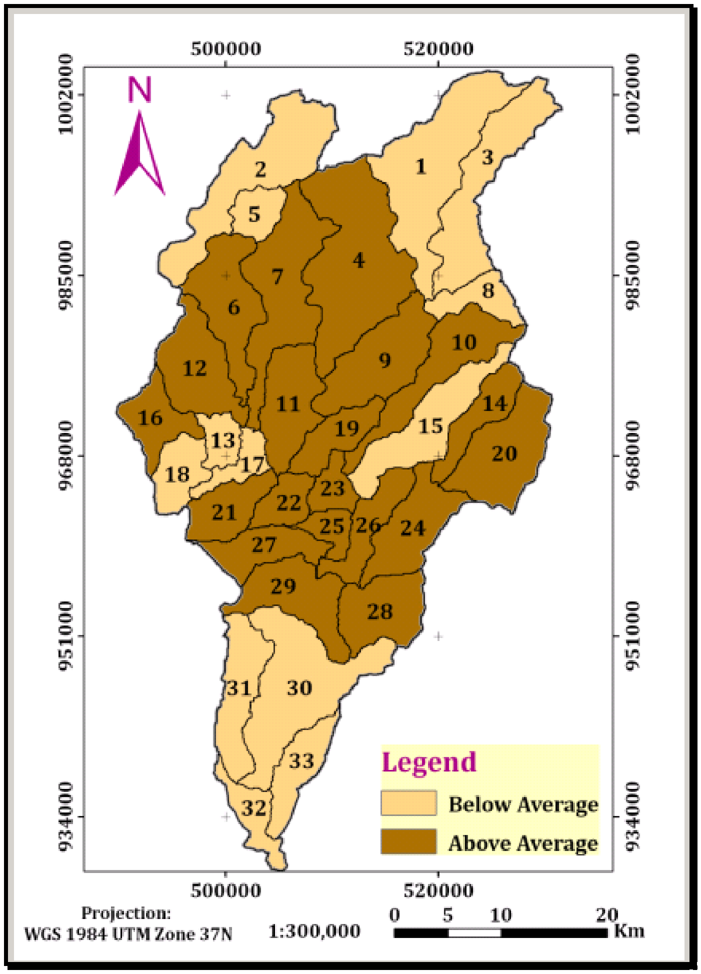


**Figure 4-6: Micro-watersheds below and above average CEI**

# 5 CONCLUSION AND RECOMMENDATIONS

## 5.1 Conclusion

GIS provides a suitable framework for the application of methods which do not have their own data management facilities for capturing, storing, retrieving, editing or displaying spatial data. Application of RUSLE model and MCA in GIS environment helps watershed managers in assessing and identifying erosion prone areas for undertaking required conservation measures. According to the results obtained discussed in previous chapter, following conclusions have been made.

Based on the RUSLE model, the total amount of potential soil loss in the Mojo River Watershed is about 9,883,473.4 tons per year from 1645.77 km$^2$. The average annual soil loss of each parcel of land in the watersheds ranges from 8.57 to 134.46t/ha/year. The mean annual soil loss of the area is 21.2t/ha/year. The result showed that very high soil loss (82.6-134.5/ha/yr) is observed in the valley as well as in the ridges of the Mojo River Watershed. Out of the 33 micro-watersheds, only one MW (MW6) experiences very high erosion rate with high contribution from C and LS factors. This MW found in the upper part of the watersheds. Six MWs (7, 9, 12, 14, 20, and 25) fell under high soil erosion classes (59.9 - 82.6t/ha/yr). Very low soil loss category (8.6- 14.7t/ha/yr) includes 2 MWs (32 and 33) which are located in the lower reach (southern part) of the study area. This may be due to the low average surface slope of less than 5% with plain topography. About 40% of the micro-watersheds fall in below the annual average soil loss of the entire watersheds.

Based on the result obtained from potential ephemeral gully identification, 94.9% (1578.81km$^2$) of the study area is with no gully and the remaining 5.1% (66.96km$^2$) is with gully erosion. In reference to land use/cover map, most of the ephemeral gullies were found in agriculture areas which are located in the upper and central parts of study area.

Based on the MCA approach, Micro-watershedwise CEI indicates that only MW 6 is under 'Very high' category with mean CEI above 2.11. The area covered under this category is 60.75 Km$^2$ (3.69%). This micro-watershed is characterized by high slope gradient. 'High' category is represented by 9 MWs (29.09%) covering 478.77 Km$^2$ area. Most parts of these micro-watersheds are under cultivated and bare land and high proportion of ephemeral gullies which causing high erosion intensity. Their location is also observed on various topographic units from ridge to valley.

## 5.2 Recommendations

The present study is mainly focus on critical (priority) area identification, and micro-watershed prioritization based on erosion risk using selected factors. Further studies can address the following issues:

- What conservation structures will be required for each erosion category classes?
- What will be the effects of anthropogenic and socioeconomic factors for critical area identification on the basis of erosion risk

Based on the result of the present study, the micro-watersheds which fall under very high and high category need immediate attention in their order of soil erosion potential. Therefore, for reducing further degradation, reclaiming the degraded areas and improving the land productivity of the watershed, and reducing their sediment delivery to low lands and reservoirs, landforms and land uses having large rate of erosion should be given first priority during the introduction of intensive and well designed SWC interventions in the study area.

## REFERENCES


Adams, J.B., Sabol, D.E., Kapos, V., Filho, R.A., Roberts, D.A., Smith, M.O., Gillespie, A. 1995. Classification of multispectral images based on fractions of endmembers: application to land-cover change in the Brazilian Amazon. *Remote Sensing of Environment* 52 (2), 137–154.

Baigorria, G. A. and Romero C. C. 2007. Assessment of erosion hotspots in a watershed: Integrating the WEPP model and GIS in a case study in the Peruvian Andes. *Environmental Modelling & Software* 22, 1175-1183

De Asis, A. M. and Omasa, K. 2007. Estimation of vegetation parameter for modeling soil erosion using linear Spectral Mixture Analysis of Landsat ETM data. ISPRS *Journal of Photogrammetry & Remote Sensing* 62, 309–324

De Asis, A. M., Omasa, K., Oki, K. and Shimizu, Y. 2008. Accuracy and applicability of linear spectral unmixing in delineating potential erosion areas in tropical watersheds. *International Journal of Remote Sensing* 29 (14), 4151 - 4171

Deore, S.J. 2005.Prioritization of Micro-watersheds of Upper Bhama Basin on the Basis of Soil Erosion Risk Using Remote Sensing and GIS Technology. PhD thesis, University of Pune, Pune.

EEPC. 2002. Koka Dam sedimentation study: Recommendations report. Ethiopian Electric Power Corporation. June 2002. Addis Ababa.

ENVI. 2002. ENVI User's Guide. Research Systems Inc., Boulder, Colorado.

Eswaran, H., Lal R. and Reich. P.F. 2001. Land degradation: an overview. In: Bridges, E.M., Hannam, I.D., Oldeman, L.R., Pening de Vries, F.W.T., Scherr, S.J. and Sompatpanit, S. (eds.). Responses to Land Degradation. International Conference on Land Degradation and Desertification. New Delhi, India.

Eyasu Elias. 2003. Case Studies: Genetic diversity, coffee and soil erosion in Ethiopia. Roles of Agriculture Project International Conference 20-22 October, 2003 Rome, Italy

FAO.1984. Ethiopian Highland reclamation Study (EHRS). Final Report, Volume 1-2. Rome.

FAO. 1986. Ethiopia Highlands Reclamation Study. Final Report, Volume 1. FAO, Rome.

FFDME. 2001. Yerer Mountain Plantation Forest Inventory and Preliminary Resource Survey.

Hawando, T. 1995. The survey of the soil and water resources of Ethiopia. NU/Toko.

Hellden, U. 1987. An Assessment of Woody Biomass, Community Forests, Land Use and Soil Erosion in Ethiopia. Lund University Press.

Hurni, H. 1985. Soil conservation manual for Ethiopia. First draft. Ministry of Agriculture, Natural Resources Conservation and Development Department, Community Forests and Soil Conservation Development Department. Addis Ababa.

Hurni, H. 1993. Land Degradation, famine and resource scenarios in Ethiopia. In World Soil Erosion and Conservation, ed. D. Pimentel. Cambridge University press, Cambridge.

Jain, S.K. and Goel, M.K. 2002. Assessing the vulnerability to soil erosion of the Ukai Dam catchments using remote sensing and GIS. *Hydrological Sciences—Journal* 47(1), 31-40

Jankowski, P. 1995. Integrating geographical information systems and multiple criteria decision making methods. *International Journal of Geographical Information Systems* 9, 251- 273.

Jetten, V., Govers, G. and Hessel, R. 2003. Erosion models: quality and spatial predictions. Hydrological Processes 17, 887-900.

Kaltenrieder. V.V.J. 2007. Adaptation and Validation of the Universal Soil Loss Equation (USLE) for the Ethiopian Eritrean Highlands. MSc, thesis. University of Bern. Switzerland.

Khan, M. A. Gupta, V.P. and Moharana, P.C. 2001. Watershed prioritization using remote sensing and geographical information system: a case study from Guhiya, India. *Journal of Arid Environments* 49, 465–475

Lal R. 1998. Agronomic consequences of soil erosion. IN: Vries F.W.T., Agus F. and Kerr J. 1998. Soil erosion at multiple scales: principles and methods for assessing causes and effects. CABI publishing. New York, USA.

Lillesand, T.M. and Kiefer, R.W. 1999. Remote Sensing and Image Interpretation. John Wiley and Sons Inc., New York.

Li, Z., O'Neill, A.L. and Lacey, S. 1996. Modelling approaches to the prediction of soil erosion in catchments. *Environmental Software* 11(1-3), 123-133.

Lu, D., Moran, E., and Batistella, M. 2003a. Linear mixture model applied to Amazonian vegetation classification. *Remote Sensing of Environment* 87, 456–469.

Lu, D., Moran, E., and Batistella, M. 2004a. Multitemporal spectral mixture analysis for Amazonian land-cover change detection. *Can. J. Remote Sensing* 30(1), 87–100.

Lu, D., Moran, E., and Batistella, M., 2004b. Application of spectral mixture analysis to Amazonian land-use and land-cover classification. *Int. J. Remote Sensing* 25(23), 5345–5358

Lulseged, T. and Vlek, P.L.G. 2005. GIS-based landscape characterization to assess soil erosion and its delivery potential in the highlands of northern Ethiopia. In Proceedings of the 1st International Conference on Remote Sensing and Geoinformation processing in the assessment and monitoring of land degradation and desertification. 7 - 9 September, Trier, Germany. 332-339.

Malczewski, J. 2004. GIS-based land-use suitability analysis: a critical overview. Progress in Planning 62, 3–65

Marti'nez-Casasnovas, J.A and Stuiver, H.G. 1998. Automated delineation of drainage network and elementary catchments from digital elevation models. *ITC journal* ¾, 198-208.

Moore,I.D,. Burch, G.J. and Mackenzie, D.H. 1988. Topographic effects on the distribution of surface soil water and the location of ephemeral gullies. *Transaction of the ASAE*. 31(4), 1098-1107.

Morgan, R.P.C. 1995. Soil Erosion and Conservation.Edinburgh: Addison-Wesley Longman.

MoWR. 2008. Awash River basin flood control and watershed management project. Feasibility report for Mojo River badlands rehabilitation. Main report

PDRE. 1989. Master plan for the Development of Surface Water Resources in the Awash Basin. Ethiopian Valleys Development Studies Authority. Final Report, Volume 6.

Petter, P. 1992. GIS and Remote Sensing for Soil Erosion Studies in Semi-arid Environments. PhD thesis. University of Lund, Lund.

Poesen, K. J., Vandaele, W. and Van Wesemael, B.1996. Contribution of gully erosion to sediment production on cultivated lands and rangelands. Erosion and Sediment Yield: Global and Regional Perspectives. In Proceedings of the Exeter Symposium July 1996. IAHS Publ. no. 236.

Poesen, J. Nachtergaele, J. Verstraeten, G. and Valentin, C. 2003. Gully erosion and environmental change: importance and research needs. *Catena* 50, 91– 133

Remortel, V. R., Hamilton, M. and Hickey, R. 2001. Estimating the LS factor for RUSLE through iterative slope length processing of digital elevation data. *Cartography,* 30(1), 27-35.

Renard, K.G., G.R. Foster, G.A. Weesies, D.K. McCool, and D.C. Yoder.1997. Predicting soil erosion by water: a guide to conservation planning with the Revised Universal Soil Loss Equation (RUSLE). Agriculture Handbook No. 703. Agricultural Research Service, Washington, DC.

Roberts, D. A., Getulio, T., Batista, Jorge, L.G., Pereira, Eric, K., Waller, and Bruce, W. 1999. Change identification using multitemporal spectral mixture analysis: Application in eastern Amazonia: in Ross S. Lunetta and Chistopher D. Elvidge; Remote Sensing Change Detection for Environmental Monitoring Methods and Application.

Saavedra, C. 2005. Estimating spatial patterns of soil erosion and deposition in the Andean region using geo-information techniques: a case study in Cochabamba, Bolivia Ph.D. dissertation, Wageningen University, The Netherlands.

Saxena, R. K., Verma, K. S., Chary, G. R., Srivastava, R. and Barthwal, A. K. 2000. IRS-1C data application in watershed characterization and Management. *Int. J. remote sensing* 21(17), 3197–3208

SCRP. 1996. Soil Erosion Hazard Assessment for Land Evaluation. University of Bern, Switzerland, in association with Ministry of Agriculture, Government of Ethiopia.

Shibru Daba, Rieger, W. and Strauss, P. 2003. Assessment of gully erosion in eastern Ethiopia using photogrammetric techniques. *Catena* 50, 273– 291

Shi Z.H., Cai C.F., Ding S.W., Wang T.W. and Chow T.L. 2003.Soil conservation planning at the small watershed level using RUSLE with GIS: a case study in the Three Gorge Area of China. *Catena* 55, 33–48

Sutcliff, J.P., 1993. Economic assessment of land degradation in the Ethiopian highlands: A case study. National conservation strategy secretariat, Ministry of planning and economic development, Addis Ababa, Ethiopia.

Tamene, L. and Vlek, P. L. G.2007.Assessing the potential of changing land use for reducing soil erosion and sediment yield of catchments: a case study in the highlands of northern Ethiopia. *Soil Use and Management* 23, 82–91

Tripathi, M.P., Panda R.K. and Raghuwanshi, N.S. 2003. Identification and prioritization of critical sub-watersheds for soil conservation management using the SWAT model. *Biosystems Engineering* 85 (3), 365–379

Vrieling, A. 2006. Satellite remote sensing for water erosion assessment: a review. *Catena* 65, 2 – 18

Wischmeier, W.H. and. Smith D.D. 1978. Predicting rainfall erosion losses: a guide to conservation planning. Agriculture Handbook No. 537. US Department of Agriculture, Washington DC.

Wolde Aragaye Berehe. 1996. Twenty years of soil conservation in Ethiopia. A personal overview. Regional Soil Conservation Unit/SIDA.

# APPENDICES

## Appendix 1: Micro-watershed wise LS factor in descending order

| Rank | Micro-watershed | Area($Km^2$) | Mean LS |
|---|---|---|---|
| 1 | 6 | 60.75 | **5.21** |
| 2 | 12 | 57.56 | **2.87** |
| 3 | 18 | 28.48 | **2.50** |
| 4 | 7 | 86.96 | **2.25** |
| 5 | 9 | 66.05 | **2.15** |
| 6 | 25 | 15.46 | **2.09** |
| 7 | 21 | 33.71 | **1.93** |
| 8 | 4 | 131.88 | **1.82** |
| 9 | 20 | 65.96 | **1.81** |
| 10 | 24 | 50.55 | **1.81** |
| 11 | 31 | 48.37 | **1.69** |
| 12 | 14 | 31.36 | **1.64** |
| 13 | 13 | 16.57 | **1.64** |
| 14 | 10 | 59.83 | **1.60** |
| 15 | 8 | 23.98 | **1.60** |
| 16 | 15 | 60.98 | **1.57** |
| 17 | 2 | 91.43 | **1.53** |
| 18 | 23 | 17.30 | **1.45** |
| 19 | 17 | 17.76 | **1.42** |
| 20 | 26 | 33.70 | **1.33** |
| 21 | 3 | 78.62 | **1.22** |
| 22 | 30 | 104.73 | **1.13** |
| 23 | 11 | 51.33 | **1.11** |
| 24 | 1 | 111.88 | **1.07** |
| 25 | 29 | 53.10 | **1.03** |
| 26 | 19 | 29.78 | **1.00** |
| 27 | 5 | 20.08 | **0.90** |
| 28 | 28 | 48.30 | **0.90** |
| 29 | 27 | 35.28 | **0.59** |
| 30 | 16 | 33.14 | **0.55** |
| 31 | 22 | 21.55 | **0.53** |
| 32 | 33 | 32.98 | **0.41** |
| 33 | 32 | 24.12 | **0.28** |

**Appendix 2: MNF and PPI image production procedures in ENVI 4.5 software (ENVI, 2002)**

***A. The Minimum Noise Fraction (MNF) transforms***

- is used to
  - determine the inherent dimensionality of image data,
  - segregate noise in the data, and
- reduce the computational requirements for subsequent processing
- is essentially two cascaded Principal Components transformations.
  - ***The first transformation***, based on an estimated noise covariance matrix, decorrelates and rescales the noise in the data. This first step results in transformed data in which the noise has unit variance and no band-to-band correlations.
  - ***The second step*** is a standard Principal Components transformation of the noise-whitened data.
- For the purposes of further spectral processing, the inherent dimensionality of the data is determined by examination of the ***final eigenvalues*** and the ***associated images***. The ***data space*** can be divided into two parts:
  - one part associated with ***large eigenvalues*** and ***coherent eigenimages***, and
  - a complementary part with ***near-unity eigenvalues*** and ***noise-dominated images***.

By using only the coherent portions, the noise is separated from the data, thus improving spectral processing results.

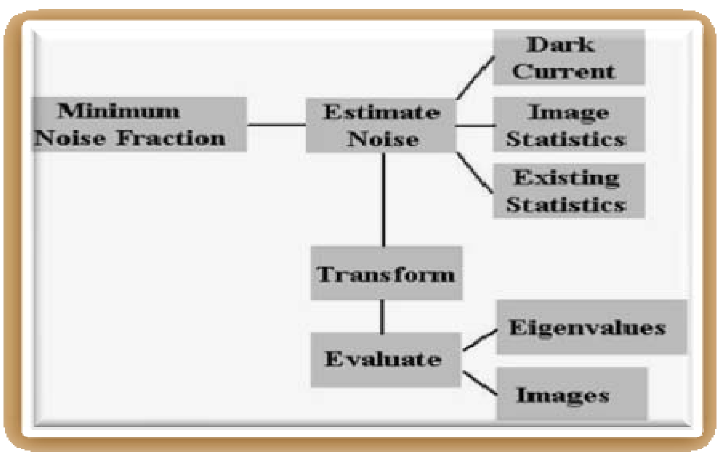


***B. The pixel purity index (PPI)***

- is a means of finding the most “spectrally pure,” or extreme, pixels in multispectral and hyperspectral images
- The PPI stipulates how many times the pixel is extreme in the simplex.
- The most spectrally pure pixels typically correspond to spectrally unique materials.
- Hence, the pixels with the highest PPI values were selected as candidate end-members as they are linearly independent in most dimensions.

- One advantage of implementing the MNF-PPI is that
    - it separates purer pixels from more mixed ones,
    - thus reducing the number of pixels to be analyzed and
    - making the separation and identification of end-members easier.

The following diagram summarizes the use of PPI in ENVI:

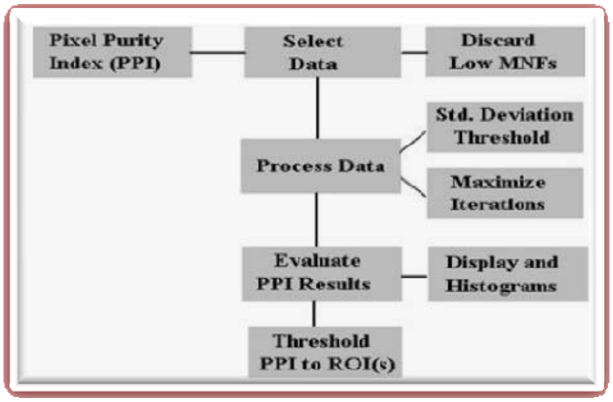

# D E C L A R A T I O N

I hereby declare that the thesis entitled "**GIS-Based Conservation Priority Area Identification in Mojo River Watershed On the Basis of Erosion Risk**" has been carried out by me under the supervision of Dr. Mekuria Argaw, Department of Environmental Sciences, Addis Ababa University, Addis Ababa during the year 2009-2010 as a part of partial fulfilment of Master of Science programme in Remote Sensing and GIS. I further declare that this work has not been submitted to any other University or Institution for the award of any degree or diploma.

Place: Addis Ababa
Date: June 2010

**Kiflu Gudeta**

# CERTIFICATE

This is to certify that the thesis entitled "**GIS-Based Conservation Priority Area Identification in Mojo River Watershed On the Basis of Erosion Risk**" is a bona-fied work carried out by Kiflu Gudeta under my guidance and supervision. This is the actual work done by Kiflu Gudeta for the partial fulfillment of the award of the Degree of Master of Science in Remote Sensing and GIS from Addis Ababa University, Addis Ababa.

***Dr. Mekuria Argaw***

*Department of Environmental Sciences*
Addis Ababa University
Addis Ababa